THE JOURNAL OF BIOLOGICAL CHEMISTRY VOL. 290, NO. 22, pp. 14245–14266, May 29, 2015

MicroRNA-26a/-26b-COX-2-MIP-2 Loop Regulates Allergic Inflammation and Allergic Inflammation-promoted Enhanced Tumorigenic and Metastatic Potential of Cancer Cells*

Received for publication, February 12, 2015, and in revised form, April 16, 2015 Published, JBC Papers in Press, April 23, 2015, DOI 10.1074/jbc.M115.645580

Yoojung Kwon[‡1], Youngmi Kim[‡1], Sangkyung Eom[‡1], Misun Kim[‡], Deokbum Park[‡], Hyuna Kim[‡], Kyeonga Noh[‡], Hansoo Lee[§], Yun Sil Lee[¶], Jongseon Choe[‖], Young Myeong Kim[‖], and Dooil Jeoung[‡2]

From the Departments of [‡]Biochemistry and [§]Biological Sciences, College of Natural Sciences, and the [‖]Graduate School of Medicine, Kangwon National University, Chunchon 200-701, Korea, and the [¶]College of Pharmacy, Ewha Womans University, Seoul 120-750, Korea

Background: The molecular mechanism of COX-2-mediated allergic inflammation remains unknown.
Results: miR-26a/-26b target COX-2 and regulate allergic inflammation-promoted enhanced tumorigenic and metastatic potential of cancer cells.
Conclusion: The miR-26a/-26b-COX-2-MIP-2 loop regulates a positive feedback between allergic inflammation and tumor metastasis.
Significance: The miR-26a/-26b-COX-2-MIP-2 loop can be employed for the development of anti-allergy and anti-cancer drugs.

Cyclooxgenase-2 (COX-2) knock-out mouse experiments showed that COX-2 was necessary for *in vivo* allergic inflammation, such as passive cutaneous anaphylaxis, passive systemic anaphylaxis, and triphasic cutaneous allergic reaction. TargetScan analysis predicted COX-2 as a target of miR-26a and miR-26b. miR-26a/-26b decreased luciferase activity associated with COX-2–3′-UTR. miR-26a/-26b exerted negative effects on the features of *in vitro* and *in vivo* allergic inflammation by targeting COX-2. ChIP assays showed the binding of HDAC3 and SNAIL, but not COX-2, to the promoter sequences of miR-26a and miR-26b. Cytokine array analysis showed that the induction of chemokines, such as MIP-2, in the mouse passive systemic anaphylaxis model occurred in a COX-2-dependent manner. ChIP assays showed the binding of HDAC3 and COX-2 to the promoter sequences of MIP-2. *In vitro* and *in vivo* allergic inflammation was accompanied by the increased expression of MIP-2. miR-26a/-26b negatively regulated the expression of MIP-2. Allergic inflammation enhanced the tumorigenic and metastatic potential of cancer cells and induced positive feedback involving cancer cells and stromal cells, such as mast cells, macrophages, and endothelial cells. miR-26a mimic and miR-26b mimic negatively regulated the positive feedback between cancer cells and stromal cells and the positive feedback among stromal cells. miR-26a/-26b negatively regulated the enhanced tumorigenic potential by allergic inflammation. COX-2 was necessary for the enhanced metastatic potential of cancer cells by allergic inflammation. Taken together, our results indicate that the miR26a/-26b-COX-2-MIP-2 loop regulates allergic inflammation and the feedback relationship between allergic inflammation and the enhanced tumorigenic and metastatic potential.

Cyclooxygenase-2 (COX-2)[3] regulates the inflammatory response induced by physiologic and stress stimuli. Allergic asthma induced by OVA involves the increased expression of COX-2 (1). Histamine regulates the expression of COX-2 through NF-κB (2). COX-2-dependent production of PGD2 mediates the dsRNA-induced enhancement of airway inflammation and responsiveness (3). TPA-induced allergic skin inflammation involves ERK activation and COX-2 up-regulation (4). MAG-EPA reduces airway hyperresponsiveness and lung inflammation in OVA-sensitized animals (5). COX-2-derived PGD2 and PGE2 regulate Th9 cell differentiation by suppressing IL-17RB expression via a protein kinase A-dependent mechanism (6). COX-2-derived PGE (2) is a hallmark of allergic inflammation. PGE synthase-1 is responsible for the conversion of COX-2-derived PGH (2) to PGE (2). Prostaglandin E synthase-1 (PGES) (2) contributes to the effector phase of some allergic responses (7). PGE (2), in autocrine or paracrine fashion, modulates transcriptional repressors of E-cadherin and thereby regulates COX-2-dependent E-cadherin expression (8). However, the role of COX-2 in allergic inflammations, such as passive cutaneous anaphylaxis (PCA), passive systemic anaphylaxis (PSA), and triphasic cutaneous allergic reaction (TpCR), remains unknown.

* This work was supported by National Research Foundation Grant 2014R1A2A2A01002448; a grant from the BK21 Plus Program; and National R&D Program for Cancer Control, Ministry for Health and Welfare, Republic of Korea Grant 1320160. This work was also supported by a grant from Kangwon National University.
[1] These authors contributed equally to this work.
[2] To whom correspondence should be addressed. Tel.: 82-33-250-8518; Fax: 82-33-259-5664; E-mail: jeoungd@kangwon.ac.kr.

[3] The abbreviations used are: COX-2, cyclooxygenase-2; DNP-HSA, 2,4-dinitrophenyl-human serum albumin; HDAC, histone deacetylase; MCP1, monocyte chemoattractant protein-1; MIP-2, macrophage inhibitory protein-2; miRNA, microRNA; PCA, passive cutaneous anaphylaxis; PSA, passive systemic anaphylaxis; qRT-PCR, quantitative RT-PCR; ROS, reactive oxygen species; TGasell, transglutaminase II; TNP, trinitrophenyl; TpCR, triphasic cutaneous reaction; TLR3, Toll-like receptor 3; HGF, hepatocyte growth factor; iNOS, inducible nitric-oxide synthase.

PSA is mediated by bioactive mediators from mast cells. PSA forms a positive feedback relationship with tumorigenesis (9, 10). These bioactive mediators cause severe hypotension, decrease in body temperature, and increased β-hexosaminidase activity (11).

Histone acetylation/deacetylation regulates various cellular processes. HDAC3 and miR-384 form a negative feedback loop and regulate allergic inflammation (10). Exposure to diesel exhaust particulate matter induces pulmonary inflammation and exacerbates asthma and chronic obstructive pulmonary disease (12). Selective degradation of HDAC1 via acetylation and the recruitment of HAT play an important role in diesel exhaust particulate matter-induced expression of the COX-2 gene (12).

The house dust extract-induced model of asthma-like pulmonary inflammation involves the induction of MIP-2 (13). Neutrophil-driven pulmonary inflammation requires MIP-2 for the recruitment of neutrophil (14). CXCR2, a receptor for MIP-2, is required for neutrophilic airway inflammation (15). Chronic production of IL-1β in respiratory epithelial cells of adult mice causes lung inflammation and airway fibrosis in the adult mouse in a manner associated with its effect on MIP-2 expression (16). The role of MIP-2 in relation to HDACs and COX-2 remains unknown.

MicroRNAs (miRNAs) are a class of small non-coding RNAs (about 22 nucleotides in length) that regulate gene expression by binding to the 3′-untranslated regions (UTRs) of target messenger RNAs (mRNAs), typically resulting in protein translation repression or mRNA degradation (17, 18). miR-146a controls nuclear factor κB-dependent inflammatory responses in keratinocytes and chronic skin inflammation in atopic dermatitis (19). miRNAs regulate mast cell development (20) and eosinophil differentiation and function (21). miR-142-3p rescues the reduction of degranulation by silencing Dicer, a key enzyme of miRNA biogenesis (22). The inhibition of miR-145 inhibits eosinophilic inflammation, mucus hypersecretion, T(H)2 cytokine production, and airway hyperresponsiveness (23). Let-7 miRNA mediates allergic lung disease by regulating the production of proinflammatory cytokines (24). Selective blockade of miR-126 suppresses the asthmatic phenotype, resulting in diminished T(H)2 responses, inflammation, airway hyperresponsiveness, eosinophil recruitment, and mucus hypersecretion (25). miR-192 targets macrophage inflammatory peptide MIP-2 in colon epithelial cells (26). These reports indicate the potential roles of miRNAs in allergic inflammation and remodeled tumor microenvironments.

In this study, we investigated the role of COX-2 in allergic inflammations, such as TpCR, PCA, and PSA. We present evidence that COX-2 is necessary for allergic inflammation *in vitro* and *in vivo*. We identified miR-26a and miR-26b as negative regulators of COX-2. We confirmed the role of miR-26a and miR-26b in allergic inflammation. We investigated the role of MIP-2, regulated by COX-2, in allergic inflammation *in vitro* and *in vivo*. We showed a negative regulatory role of miR-26a and miR-26b in the positive feedback relationship between allergic inflammation and the enhanced tumorigenic and metastatic potential. We showed that COX-2 was necessary for allergic inflammation-promoted enhanced metastatic potential of cancer cells. The miR-26a/-26b-COX-2-MIP-2 loop regulated allergic inflammation and the relationship between allergic inflammation and the enhanced tumorigenic and metastatic potential. Thus, the COX-2-miR-26a/-26b-MIP-2 loop is a potential target for the development of anti-allergy and anti-cancer drugs.

Experimental Procedures

β-Hexosaminidase Activity Assays—The β-hexosaminidase activity assay was performed according to standard procedures (9).

Cell Lines and Cell Culture—RBL2H3 (rat basophilic leukemia) cells were obtained from the Korea Cell Line Bank (Seoul, Korea). Cells were grown in Dulbecco's modified Eagle's medium containing heat-inactivated fetal bovine serum, 2 mM L-glutamine, 100 units/ml penicillin, and 100 μg/ml streptomycin (Invitrogen). Cultures were maintained in 5% CO_2 at 37 °C. Bone marrow-derived mouse mast cells were isolated and cultured according to standard procedures (24). B16F1 and B16F10 melanoma cells were cultured in Dulbecco's modified minimal essential medium (DMEM; Gibco) supplemented with heat-inactivated 10% fetal bovine serum (FBS; Gibco) and antibiotics at 37 °C in a humidified incubator with a mixture of 95% air and 5% CO_2. Lung macrophages and lung endothelial cells were isolated according to the standard procedures (10).

Isolation of Ear Skin Mast Cells from Mice—Ears of BALB/c mice were cut into fragments and incubated in RPMI 1640 medium supplemented with 25% fetal bovine serum, 1.5 mg/ml collagenase (Sigma-Aldrich), 0.5 mg/ml hyaluronidase (Sigma-Aldrich), 0.2 mg/ml protease (Sigma-Aldrich), and 0.5 mg/ml DNase I (Sigma-Aldrich) for 60 min at 37 °C. Dispersed cells were filtered sequentially through 70- and 40-μm cell strainers (BD Biosciences). The pelleted cells were resuspended in RPMI 1640 medium containing 0.1% bovine serum albumin and submitted to a continuous isotonic Percoll gradient (72%) for mast cell isolation. Purified mast cells were resuspended in RPMI-FBS. The cell purity (>96%) and viability (>98%) were evaluated by toluidine blue and trypan blue exclusion staining, respectively.

Isolation of Lung Mast Cells—Lung tissues of BALB/c mice were cut into fragments and incubated in modified Tyrode's buffer (137 mmol/liter NaCl, 2.8 mmol/liter KCl, 12 mmol/liter $NaHCO_3$, 0.49 mmol/liter $MgCl_2$, 0.4 mmol/liter NaH_2PO_4, 5.5 mmol/liter glucose, 10 mmol/liter HEPES, 3.5 mg/ml BSA) medium supplemented with 0.5 mg/ml collagenase (Sigma-Aldrich) for 15 min at 37 °C. The supernatant tissue pellets were collected and resuspended with collagenase solution in Tyrode's buffer at 37 °C for another 30 min. After 30 min, 10 ml of 0.015 mg/ml DNase I (Sigma-Aldrich) solution in PBS was added to tissue pellet and incubated at 37 °C for another 30 min. To remove the large undigested tissue pieces, the tissue pellets were filtered through 70-μm strainers (BD Biosciences). The pelleted cells were resuspended in lysis buffer (1.37 g of NH_4Cl, 0.515 g of Tris, 250 ml of double-distilled H_2O, pH 7.2) to remove red blood cells and incubated for 5 min at room temperature. After the addition of 10 ml of PBS/DNase solution to stop the lysis reaction and centrifugation at 200 × g for 10 min, the cell pellets were resuspended in DNase I solution in RPMI

medium and subjected to a continuous isotonic Percoll gradient (72%). Purified mast cells were resuspended in RPMI-FBS. The cell purity (>96%) and viability (>98%) were evaluated by toluidine blue and trypan blue exclusion staining, respectively.

Mice—Five-week-old female BALB/c mice were purchased from Nara Biotech (Seoul, Korea) and maintained in specific pathogen-free conditions. All animal experiments were approved by the Institutional Animal Care and Use Committee of Kangwon National University (KW-140707-1). To measure the tumorigenic potential, mouse melanoma B16F1 cells (1×10^6 cells in 100 μl of PBS), after induction of passive systemic anaphylaxis, were injected subcutaneously into the right flank of each mouse ($n = 5$). Tumor growth was evaluated by measuring the tumor diameters with calipers and calculating the tumor volumes using an approximated formula for a prolate ellipsoid as follows, volume $= ((a \times b^2)/2)$, where a is the longest axis of the tumor, and b is the shortest axis. After 3 weeks, the mice were sacrificed, and the final tumor volumes were measured. To determine the effect of miR-26 on the tumorigenic potential, miR-26a mimic (100 nM) or miR-26 mimic (100 nM) was injected intravenously five times, before and after B16F1 cell injection, in a total of 17 days. COX-2(−/−) mice were kindly provided by professor Young Myeong Kim (Kangwon National University, Korea).

Chemicals and Reagents—Oligonucleotides used in this study were commercially synthesized by the Bionex Company (Seoul, Korea). Chemicals used in this study were purchased from Sigma. DNP-HSA and DNP-specific IgE antibody were purchased from Sigma. TNP-BSA was purchased from Santa Cruz Biotechnology. TNP-specific IgE antibody was purchased from BioLegend Co. Anti-mouse and anti-rabbit IgG-horseradish peroxidase conjugate antibody was purchased from Pierce. All other antibodies were purchased from Cell Signaling Co. (Beverly, MA). Lipofectamine and Plus™ reagent for transfection were purchased from Invitrogen. Cytokine array kit was purchased from (R&D Systems, Minneapolis, MN). miR mimics and miR inhibitors were purchased from Bioneer Company (Daejon, Korea).

Transfection—Transfections were performed according to the manufacturer's instructions. Lipofectamine and Plus reagents (Invitrogen) were used. The construction of siRNA was carried out according to the instruction manual provided by the manufacturer (Ambion, Austin, TX). For miR-26 knockdown, cells were transfected with 10 nM oligonucleotide (inhibitor) with Lipofectamine 2000 (Invitrogen), according to the manufacturer's protocol. The sequences used were as follows: 5′-AGCCUAUCCUGGAUUACUUGAA-3′ (miR-26a inhibitor) and 5′-GCAUCUAUCUAUAUAUCUA-3′ (control inhibitor); 5′-AAGUUCAUUAAGUCCUAUCCAA-3′ (miR-26b inhibitor) and 5′-GCAUCUAUCUAUAUAUCUA-3′ (control inhibitor).

ChIP Assay—Assays were performed according to the manufacturer's instructions (Upstate Biotechnology, Inc.). The antibody immunoprecipitates were reverse cross-linked. PCR was done on the phenol-chloroform-extracted DNA with specific primers. To examine the binding of protein of interest to the *miR-26a* promoter sequences, specific primers of the *miR-26a* promoter-1 sequences (5′-CCACACTCCCTGGGAACATC-3′ (sense) and 5′-TGCATGCATGAGGCAGAGAA-3′ (antisense)), *miR-26a* promoter-2 sequences (5′-TCCCCCATCAAACTCAAGGC-3′ (sense) and 5′-GGAAAGAGCCCTGGCTTAGG-3′ (antisense)), and *miR-26a* promoter-3 sequences (5′-ACCTAGCTCTCTATCCTGTCCT-3′ (sense) and 5′-GGGTGTCTACTGCCAAAGAGAA-3′ (antisense)) were used.

To examine the binding of protein of interest to the *miR-26b* promoter sequences, specific primers of the *miR-26b* promoter-1 sequences (5′-GACCTAGCCGGAAGTAGACTTG-3′ (sense) and 5′-TGAAGGAGCTGTGCACCA-3′ (antisense)), *miR-26b* promoter-2 sequences (5′-TGGTGCACAGCTCCTTCA-3′ (sense) and 5′-TAGTGCAGACACCAAGCTCC-3′ (antisense)), and *miR-26b* promoter-3 sequences (5′-GGAGCTTGGTGTCTGCACTA-3′ (sense) and 5′-GTAGGGGTAAGAGGGGAAAGA-3′ (antisense)) were used.

To examine the binding of protein of interest to MIP-2 promoter sequences, specific primers of the *MIP-2* promoter-1 sequences (5′-AAGAGCCTCGGAAGTTCC-3′ (sense) and 5′-TGTGTGTTCAAGCGTGAAC-3′ (antisense)) and MIP-2 promoter-2 sequences (5′-GTTCACGCTTGAACACACA-3′ (sense) and 5′-TCTGAGGTCCCGAGAGCT-3′ (antisense)) were used.

miR-26a, miR-26b, and pGL3–3′-UTR-COX-2 Construct—To generate miR-26a expression vector, a 412-bp genomic fragment encompassing the primary miR-26a gene was PCR-amplified and cloned into the GGATCC ↓ CTCGAG site of the pcDNA3.1 vector. To generate miR-26b expression vector, a 330-bp genomic fragment encompassing the primary miR-26b gene was PCR-amplified and cloned into the GGATCC ↓ CTCGAG site of pcDNA3.1 vector. To generate the pGL3–3′-UTR-COX-2 construct, a 567-bp mouse COX-2 gene segment encompassing 3′-UTR was PCR-amplified and subcloned into the TCTAGA ↓ TCTAGA site of the pGL3 luciferase plasmid. The mutant pGL3–3′-UTR-COX-2 construct was made with deletion of the miR-26a- or miR-26b-responsive element. The luciferase activity assay was performed according to the instruction manual (Promega).

IgE-dependent TpCR in Mouse Ear—To induce the IgE-dependent TpCR in the ear of female BALB/C mice, mice were sensitized by injecting DNP-specific IgE antibody (10 μg/kg) intravenously. Twenty-four hours later, a cutaneous reaction was evoked by painting with 25 μl of 0.15% 2,4-dinitrofluorobenzene acetone/olive oil (3:1) solution onto each surface of both ear lobes. Ear thickness was measured by using a digital gauge.

Passive Cutaneous Anaphylaxis—BALB/C mice were passively sensitized with an intradermal injection of DNP-specific IgE (0.5 μg/kg). The mice were challenged 24 h later with an intravenous injection of DNP-HSA (250 μg/kg) plus 250 μl of PBS containing 2% (v/v) Evans Blue solution. Thirty minutes after DNP-HSA challenge, the mice were euthanized, and the 2% (v/v) Evans Blue dye was extracted from each dissected ear in 700 μl of acetone/water (7:3) overnight. The absorbance of Evans Blue in the extracts was measured with a spectrophotometer at 620 nm. To determine the effect of miR-26 on the PCA, BALB/C mice were given an intravenous injection of control mimic (100 nM) or miR-26a mimic (100 nM) on the next day of

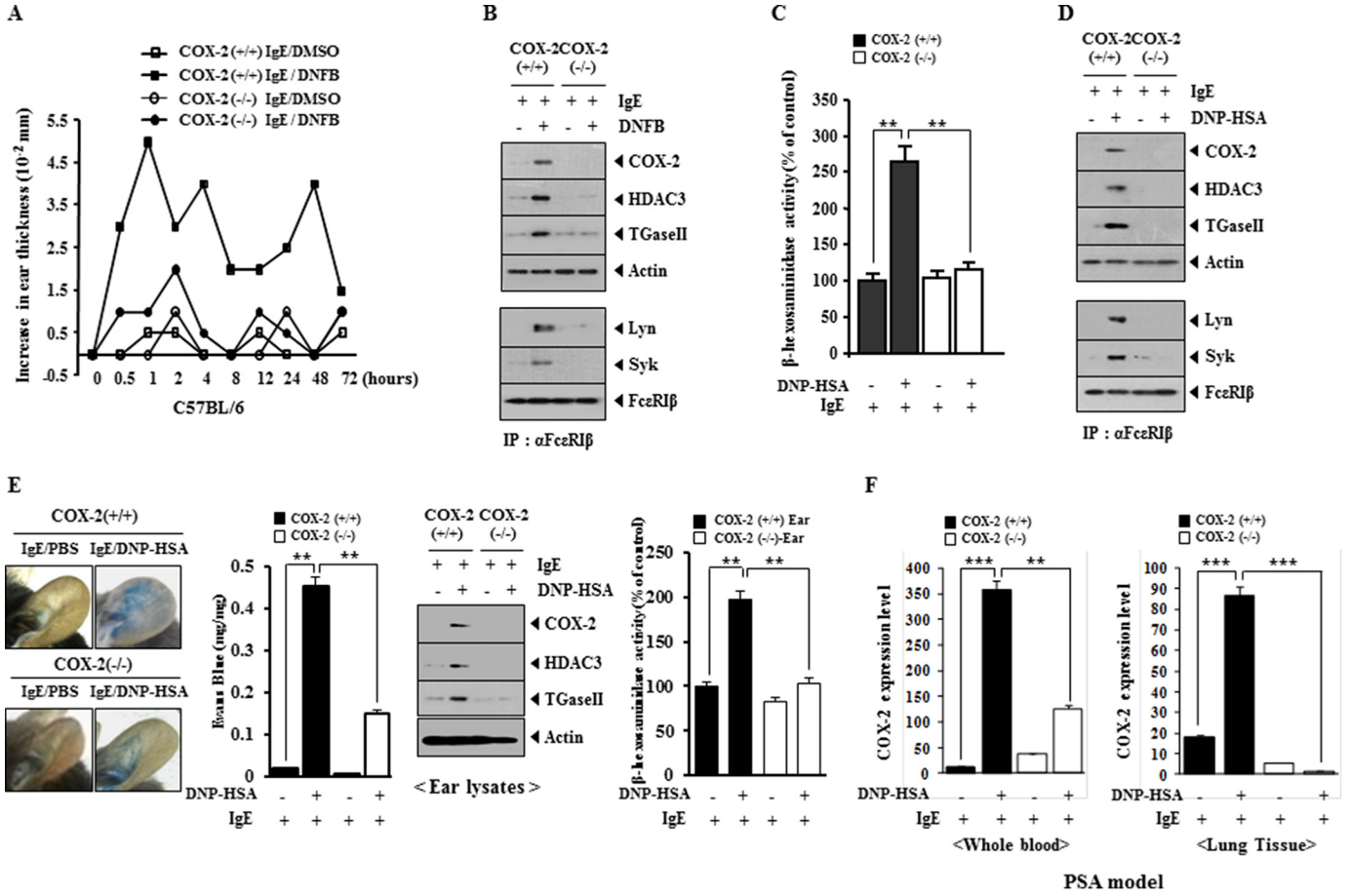

FIGURE 1. **COX-2 is necessary for *in vivo* allergic inflammation.** *A*, the indicated C57BL/6 mice were sensitized to DNP-specific IgE (0.5 μg/kg) by an intravenous injection. The next day, both ears of mice were painted with 2,4-dinitrofluorobenzene (*DNFB*) or DMSO. At each time point after 2,4-dinitrofluorobenzene stimulation, ear thickness was measured. Each experimental group consisted of five mice. Means ± S.E. (*error bars*) of three independent experiments are shown. *B*, ear tissue lysates isolated from each mouse were subjected to Western blot analysis (*top*) immunoprecipitation (*IP*) with the indicated antibody (2 μg/ml), followed by Western blot analysis (*bottom*). *C*, cell lysates isolated from ear skin mast cells of each mouse were subjected to β-hexosaminidase activity assays. **, $p < 0.005$. *D*, lysates isolated from ear skin mast cells of each mouse were subjected to Western blot analysis (*top*) and were immunoprecipitated with the indicated antibody, followed by Western blot analysis (*bottom*). *E*, PCA employing the C57BL/6 mice was performed as described. In brief, the indicated C57BL/6 mice were given an intradermal injection of DNP-specific IgE antibody (0.5 μg/kg) or DNP-specific IgG (0.5 μg/kg). The next day, the mice were given an intravenous injection of PBS or DNP-HSA (250 μg/kg) along with 2% (v/v) Evans Blue solution. One hour after the injection, the extent of vascular permeability was determined as described. Each experimental group consisted of four mice. Means ± S.E. of three independent experiments are depicted. Representative images from four animals of each experimental group are shown. Ear tissue lysates isolated from each mouse were subjected to Western blot analysis and β-hexosaminidase activity assays. **, $p < 0.005$. *F*, PSA employing the indicated C57BL/6 mice was performed. In brief, the indicated C57BL/6 mice were sensitized to DNP-specific IgE (0.5 μg/kg) by an intravenous injection. The next day, the indicated mice were given an intravenous injection of DNP-HSA (250 μg/kg). The mRNAs from whole blood and lung tissues were isolated and subjected to qRT-PCR analysis. **, $p < 0.005$; ***, $p < 0.0005$.

the sensitization with DNP-specific IgE. One hour after the injection of miR mimic, BALB/c mice were challenged with DNP-HSA (250 μg/kg) plus 250 μl of PBS containing 2% (v/v) Evans Blue solution for determining the extent of vascular permeability accompanied by PCA.

IgE-dependent Passive Systemic Anaphylaxis—For the induction of passive systemic anaphylaxis, BALB/c mice were sensitized by an intravenous injection of DNP-specific IgE (0.5 μg/kg) or TNP-specific IgE (0.5 μg/kg). The next day, sensitized mice were challenged by an intravenous injection of DNP-HSA (250 μg/kg) or TNP-BSA (250 μg/kg). To examine the effect of miR-26a or miR-26b on PSA, BALB/c mice were passively sensitized with an intravenous injection of DNP-specific IgE (0.5 μg/kg) or TNP-specific IgE (0.5 μg/kg) along with miR-26a mimic (100 nM) or miR-26b mimic (100 nM). The mice were challenged 24 h later with an intravenous injection of DNP-HSA (250 μg/kg) or TNP-BSA (250 μg/kg).

Monitoring of Rectal Temperature—Changes in core body temperature associated with systemic anaphylaxis were monitored by measuring changes in rectal temperatures using a rectal probe coupled to a digital thermometer as described (9, 10).

Cytokine Arrays—Expression levels of cytokine/chemokines were determined by using a Proteom Profiler™ mouse cytokine array kit (R&D Systems, Minneapolis, MN) according to the manufacturer's instructions.

Reactive Oxygen Species (ROS) Measurement—The IgE-sensitized RBL2H3 cells were transfected with control vector (1 μg), miR-26a (1 μg), or miR-26b (1 μg) for 24 h, followed by stimulation with DNP-HSA (100 ng/m) for 1 h. The level of reactive oxygen species was measured by using the 2′,7′-dichlorofluorescein diacetate by confocal microscopy.

Rac1 Activity—Rac1 activity assays were performed according to well established procedures (27).

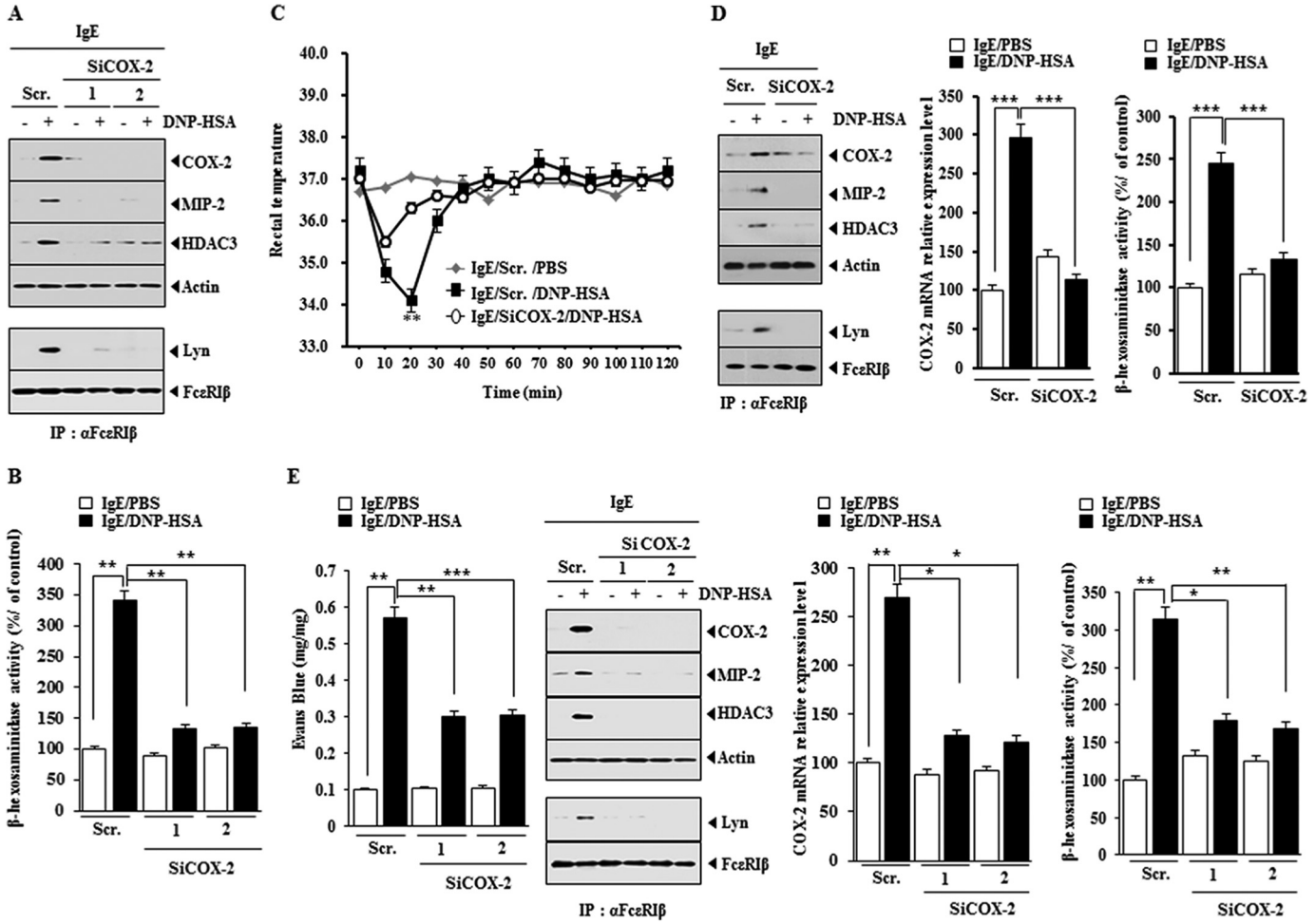

FIGURE 2. **The down-regulation of COX-2 negatively regulates allergic inflammation *in vitro* and *in vivo*.** *A*, RBL2H3 cells were transfected with the indicated siRNA (each at 10 nM) prior to sensitization with DNP-specific IgE (100 ng/ml). The IgE-sensitized RBL2H3 cells were then stimulated with DNP-HSA (100 ng/ml) for 1 h. Cell lysates were subjected to Western blot analysis. *IP*, immunoprecipitation; *Scr.*, scrambled siRNA. *B*, same as *A* except that β-hexosaminidase activity assays were performed. **, $p < 0.005$. *C*, BALB/c mice were injected with scrambled (100 nM) or COX-2 siRNA (100 nM) via the tail vein. The next day, BALB/c mice were injected with DNP-specific IgE (0.5 μg/kg) via the tail vein. The following day, BALB/c mice were injected intravenously with DNP-HSA (250 μg/kg) or PBS, and rectal temperatures were measured. Each experimental group consisted of five mice. The means ± S.E. (*error bars*) of three independent experiments are depicted. *D*, 2 h after the injection of DNP-HSA, lung tissue lysates were isolated and subjected to Western blot analysis. Lung tissue lysates were also immunoprecipitated with the indicated antibody, followed by Western blot analysis. Lung tissue lysates were also subjected to qRT-PCR analysis and β-hexosaminidase activity assays. ***, $p < 0.0005$. *E*, BALB/c mice were given an intradermal injection of DNP-specific IgE (0.5 μg/kg). The next day, BALB/c mice were given an intravenous injection of scrambled (100 nM) or COX-2 siRNA (100 nM). One hour after the injection of siRNA, BALB/c mice were given an intravenous injection of PBS or DNP-HSA (250 μg/kg) along with 2% (v/v) Evans Blue solution. One hour after the injection of Evans Blue solution, the dye was eluted from the ear in 700 μl of formamide at 63 °C. The absorbance was measured at 620 nm. Ear lysates were subjected to β-hexosaminidase activity assays, qRT-PCR analysis, immunoprecipitation, and Western blot. *, $p < 0.05$; **, $p < 0.005$; ***, $p < 0.005$.

RNA Extraction and Quantitative RT-PCR (qRT-PCR)—Total miRNA was isolated using the *mir*Vana miRNA isolation kit (Ambion). miRNA was extended by a poly(A) tailing reaction using the A-Plus poly(A) polymerase tailing kit (Cell Script). cDNA was synthesized from miRNA with a poly(A) tail using a poly(T) adaptor primer and qScript™ reverse transcriptase (Quanta Biogenesis). Expression levels of miR-26a or miR-26b were quantified with the SYBR Green qRT-PCR kit (Ambion) using a miRNA-specific forward primer and a universal poly(T) adaptor reverse primer. The expression of miR-26a or miR-26b was defined based on the threshold (*Ct*), and relative expression levels were calculated as $2^{-((Ct \text{ of miR-26a or miR-26b}) - (Ct \text{ of U6}))}$ after normalization with reference to expression of U6 small nuclear RNA. For quantitative PCR, SYBR PCR Master Mix (Applied Biosystems) was used in a CFX96 real-time system thermocycler (Bio-Rad). To determine the level of COX-2 or MIP-2 mRNA, total RNA was isolated with TRIzol reagent (Invitrogen). RNA was then reverse transcribed using Moloney murine leukemia virus reverse transcriptase (Invitrogen) and random primers (Roche Applied Science). The cDNA was amplified with specific primers and Power SYBR Green PCR master mix (Applied Biosystems).

Preparation of siRNA Duplexes—Construction of siRNA was carried out according to the instruction manual provided by the manufacturer (Ambion, Austin, TX). *COX-2* siRNA-1 sequences (5′-AATTTCCCTTCACACCCATGGCCTCTTCTC-3′ (sense) and 5′-AACCATGGGTGTGAAGGGAAACCTGTCTC-3′ (antisense)); *COX-2* siRNA-2 sequences (5′-GACUACGUGCAACACCUGACCTGTCTC-3′ (sense) and 5′-UCAGGUGUUGCACGUAGUCCCTGTCTC-3′ (antisense)); COX-2 scrambled (5′-GTTCTCCCACCCGTACTTCAACCTAGTCT-3′

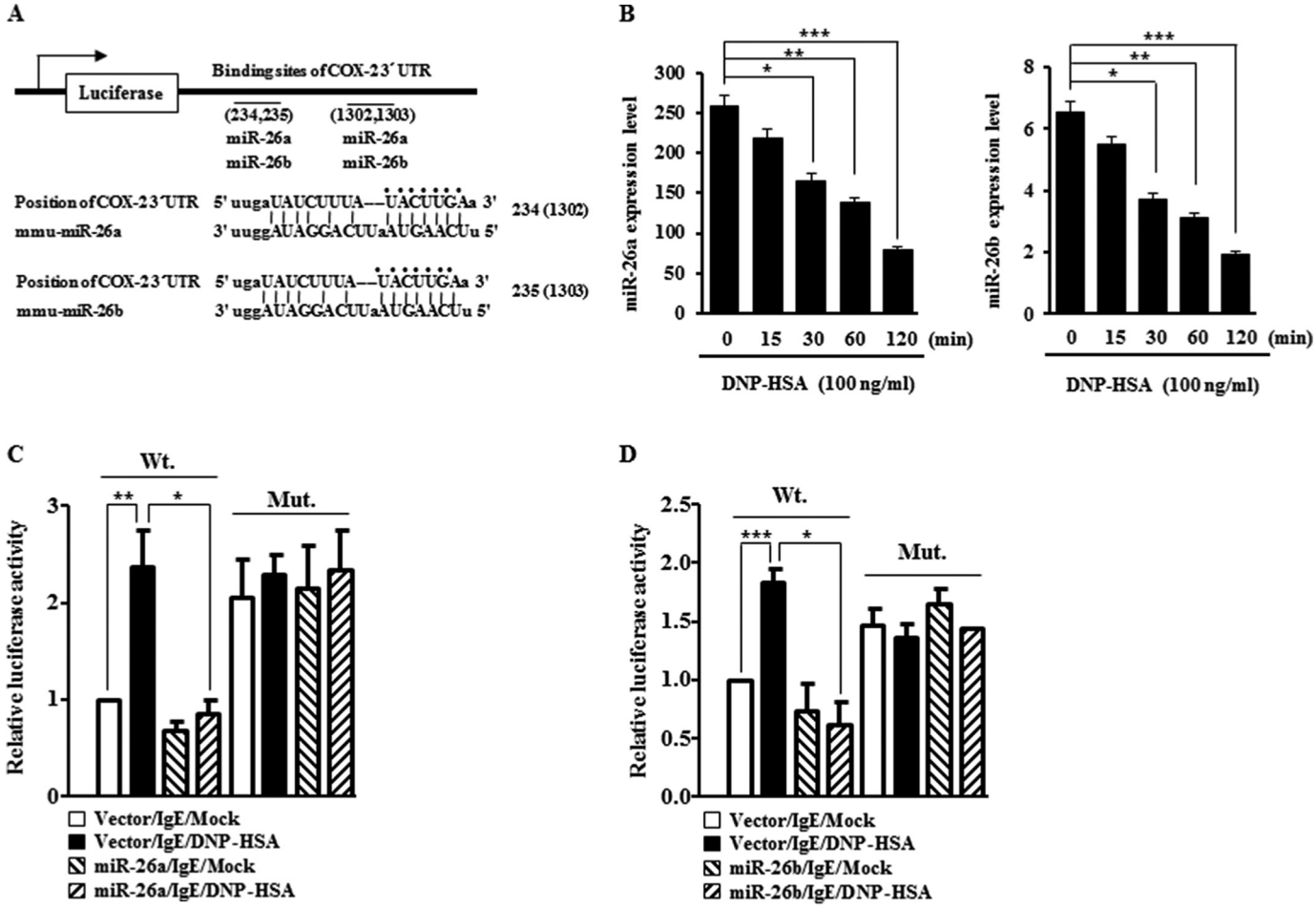

FIGURE 3. **miR-26a and miR-26b target COX-2.** *A*, potential binding of miR-26a and miR-26b to the 3′-UTR of COX-2. *B*, the IgE-sensitized RBL2H3 cells were stimulated with DNP-HSA (100 ng/ml) for various time intervals. miRNA isolated at each time point was subjected to qRT-PCR. *, $p < 0.05$; **, $p < 0.005$; ***, $p < 0.0005$. *C*, RBL2H3 cells were transfected with control vector (1 μg) or miR-26a construct (1 μg) along with wild type 3′-COX-2- UTR-luciferase construct or mutant 3′-COX-2-UTR-luciferase construct (*Mut.*) prior to sensitization with DNP-specific IgE (100 ng/ml). The IgE-sensitized RBL2H3 cells were then stimulated with DNP-HSA (100 ng/ml) for 1 h. Luciferase activity assays were performed as described. *, $p < 0.05$; **, $p < 0.005$. *D*, same as *C* except that miR-26b construct (1 μg) was transfected into RBL2H3 cells. *, $p < 0.05$; ***, $p < 0.0005$. *Error bars*, S.E.

(sense) and 5′-GAACGGGTCTGCACTAGGAGCCATAAGTT-3′ (antisense)); *MIP-2* siRNA-1 sequences (5′-GAGUUGGGAACUAGCUACA-3′ (sense) and 5′-UGUAGCUAGUUCCCAACUC-3′ (antisense)); *MIP-2* siRNA-2 sequences (5′-GUGAGUAACCCUUGGACAUCCTGTCTC-3′ (sense) and 5′-AUGUCCAAGGGUUACUCACCCTGTCTC-3′ (antisense)); MIP-2 scrambled (5′-GGTACGTCTCGAAGATAGA-3′ (sense) and 5′-GCTATCGCCCATTGCTAAT-3′ (antisense)) were used.

Western Blot Analysis—Western blot and immunoprecipitation were performed according to standard procedures (10). For analysis of proteins from tissues, frozen samples were ground to a fine powder using a mortar and pestle over liquid nitrogen. Proteins were solubilized in radioimmune precipitation buffer containing protease inhibitors, and insoluble material was removed by centrifugation.

miRNA Target Analysis—Genes that contain the miR-binding site(s) in the UTR were obtained using the TargetScan program.

Intravital Microscopy—Male BALB/c mice (6–8 weeks old) were obtained from Daehan Biolink. *In vivo* angiogenesis was assessed as follows. The mice were anesthetized with 2.5% avertin (v/v) via intraperitoneal injection (Surgivet), and abdominal wall windows were implanted. Next, a titanium circular mount with eight holes on the edge was inserted between the skin and the abdominal wall. Growth factor-reduced Matrigel containing the conditioned medium was applied to the space between the windows, and a circular glass coverslip was placed on top and fixed with a snap ring. After 4 days, the animals were anesthetized and injected intravenously with 50 μl of 25 ng/ml fluorescein isothiocyanate-labeled dextran (M_r ~2,000,000) via the tail vein. The mice were then placed on a Zeiss Axiovert 200M microscope. The epi-illumination microscopy setup included a 100-watt mercury lamp and filter set for blue light. Fluorescence images were recorded at random locations of each window using an electron-multiplying charge-coupled device camera (Photo Max 512, Princeton Instruments) and digitalized for subsequent analysis using the Metamorph program (Universal Imaging). The assay was scored from 0 (negative) to 5 (most positive) in a double-blinded manner. To determine the effect of miR mimics on the PSA-promoted angiogenesis, BALB/c mice were sensitized to DNP-specific IgE (0.5 μg/kg) by an intravenous injection. BALB/C mice were also given an intravenous injection of control mimic (100 nM), miR-26a mimic (100 nM), or miR-26b mimic (100 nM). The next day,

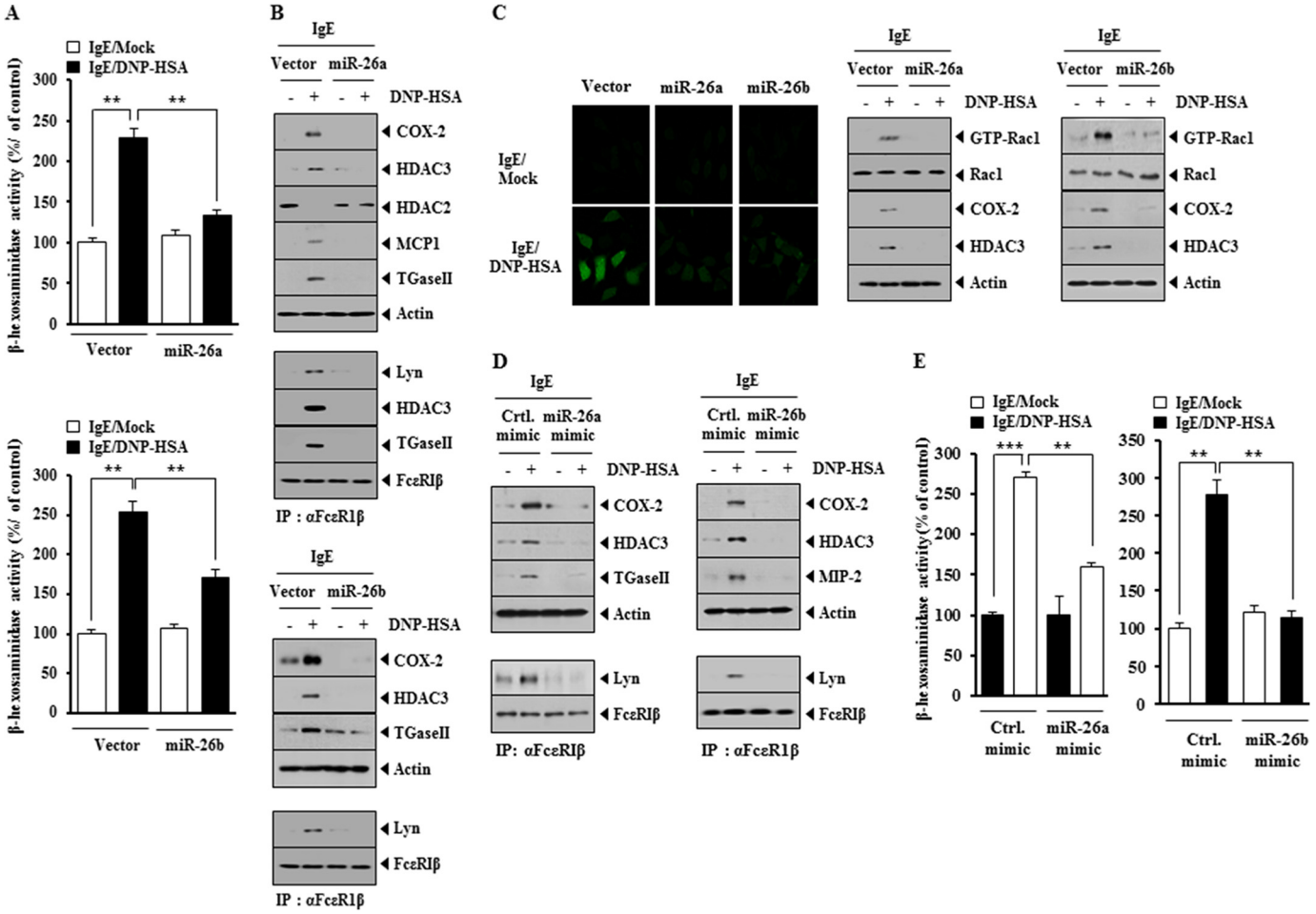

FIGURE 4. **miR-26a and miR-26b negatively regulate the *in vitro* allergic inflammation.** *A*, RBL2H3 cells were transfected with control vector (1 μg), miR-26a construct (1 μg), or miR-26b construct (1 μg) prior to sensitization with DNP-specific IgE (100 ng/ml). The IgE-sensitized RBL2H3 cells were then stimulated with DNP-HSA (100 ng/ml) for 1 h. Cell lysates were subjected to β-hexosaminidase activity assays. **, $p < 0.005$. *B*, same cell lysates were subjected to Western blot analysis (*top*). Cell lysates were also subjected to immunoprecipitation (*IP*) employing the indicated antibody, followed by Western blot analysis (*bottom*). *C*, the level of reactive oxygen species was measured by employing DCFH-DA (*left*). Rac1 activity assays employing cell lysates were performed as described (*right*). *D*, RBL2H3 cells were transfected with control mimic (10 nM), miR-26a mimic (10 nM), or miR-26b mimic (10 nM) prior to sensitization with DNP-specific IgE (100 ng/ml). The IgE-sensitized RBL2H3 cells were then stimulated with DNP-HSA (100 ng/ml) for 1 h. Cell lysates were subjected to Western blot analysis (*top*). Cell lysates were also subjected to immunoprecipitation (*IP*) employing the indicated antibody, followed by Western blot analysis (*bottom*). *E*, same as *D* except that β-hexosaminidase activity assays were performed. **, $p < 0.005$; ***, $p < 0.0005$. *Error bars*, S.E.

BALB/c mice were given an intravenous injection of DNP-HSA (250 μg/kg) or PBS. One hour after stimulation with DNP-HSA (250 μg/kg), lung tissues were isolated. Lung mast cells were then isolated. The conditioned medium of lung mast cells (10 μl) was mixed with growth factor-reduced Matrigel. Intravital microscopy was performed as described.

In Vivo Matrigel Plug Assay—Seven-week-old BALB/c mice (DBL Co., Ltd., Seoul, Korea) were injected subcutaneously with 0.1 ml of Matrigel containing the conditioned medium and 10 units of heparin (Sigma). The injected Matrigel rapidly formed a single, solid gel plug. After 8 days, the skin of the mouse was easily pulled back to expose the Matrigel plug, which remained intact. Hemoglobin content in the Matrigel plugs was measured using the Drabkin reagent (Sigma) for quantification of blood vessel formation. To determine the effect of miR-26 on the angiogenic potential, the conditioned medium of lung mast cells, obtained after PSA induction in the absence or presence of miR-26a mimic or miR-26b mimic, was mixed with Matrigel containing 10 units of heparin.

Histological Analyses—Immunohistochemical staining of lung tissues was also performed using an established avidin-biotin detection method (Vectastain ABC kit, Vector Laboratories Inc., Burlingame, CA). Briefly, 4–6-μm-thick sections of the paraffin-embedded tissue blocks were cut, mounted on positively charged glass slides, and dried in an oven at 56 °C for 30 min. The sections were deparaffinized in xylene and then rehydrated in graded ethanol and water. Endogenous peroxidase was blocked by incubation in 3% (v/v) hydrogen peroxide for 15 min. Antigen retrieval was accomplished by pretreatment of the sections with citrate buffer at pH 6.0 for 20 min at 56 °C in a microwave oven and then allowing the sections to cool for 30 min. Nonspecific endogenous protein binding was blocked using 1% bovine serum albumin (BSA). The sections were then incubated with primary antibodies overnight at 4 °C. The following primary antibodies were used for single and double staining: anti-MIP-2 (1:100; Santa Cruz Biotechnology) and anti-COX-2 (1:50; Abcam). After washing, biotinylated secondary antibodies were applied at 1:100 or 1:200 dilutions

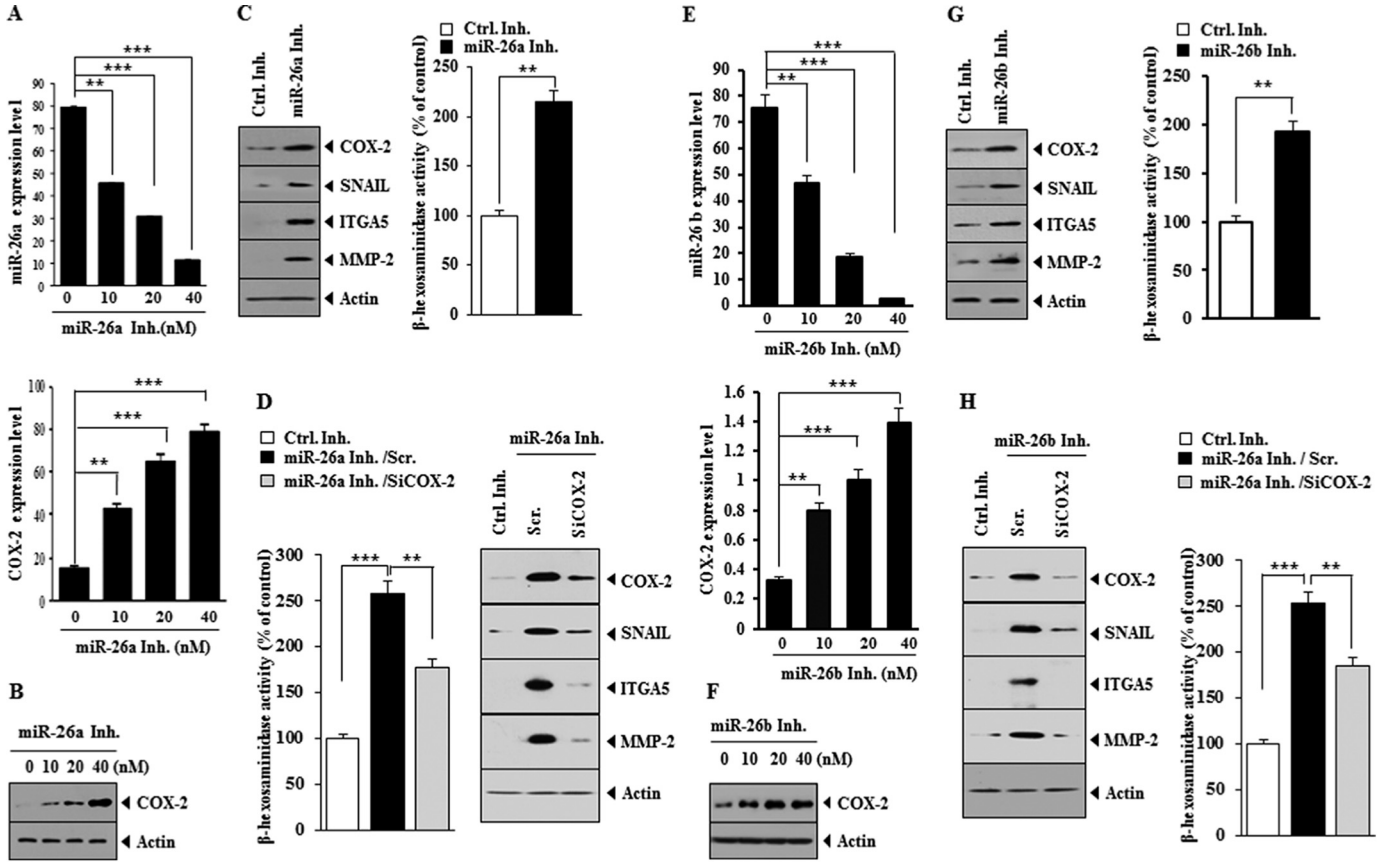

FIGURE 5. **miR-26a inhibitor and miR-26b inhibitor target COX-2 to regulate *in vitro* allergic inflammation.** *A*, RBL2H3 cells were treated with various concentrations of miR-26a inhibitor for 8 h. qRT-PCR analysis for determination of expression level of miR-26a and COX-2 mRNA was performed. **, $p < 0.005$; ***, $p < 0.0005$. *B*, RBL2H3 cells were treated with various concentrations of miR-26a inhibitor for 8 h. Cell lysates were subjected to Western blot analysis. *C*, RBL2H3 cells were transfected with the indicated inhibitor (each at 10 nM). At 24 h after transfection, cell lysates were prepared and subjected to Western blot analysis. *C*, RBL2H3 cells were treated with the indicated inhibitor (10 nM each) for 8 h. Cell lysates were subjected to β-hexosaminidase activity assays. **, $p < 0.005$. *D*, RBL2H3 cells were transfected with the indicated inhibitor (10 nM) along with the indicated siRNA (10 nM). At 48 h after transfection, cell lysates were subjected to Western blot analysis and β-hexosaminidase activity assays. **, $p < 0.005$; ***, $p < 0.0005$. *E*, same as *A* except that RBL2H3 cells were treated with various concentrations of miR-26b inhibitor for 8 h. **, $p < 0.005$; ***, $p < 0.0005$. *F*, same as *B* except that RBL2H3 cells were transfected with miR-26b inhibitor (10 nM). *G*, same as *C* except that RBL2H3 cells were treated with miR-26b inhibitor (10 nM) for 8 h. **, $p < 0.005$. *H*, same as *D* except that RBL2H3 cells were transfected with miR-26b inhibitor (10 nM). **, $p < 0.005$; ***, $p < 0.0005$. *Error bars*, S.E.

for 1 h. Color was developed with diaminobenzidine (Vector Laboratories, Inc.). Sections were counterstained with Mayer's hematoxylin. Sections incubated without primary antibody served as controls. To visualize tissue mast cells, the sections were stained with 0.1% olivine blue (Sigma) in 0.1 N HCl for 15 min.

In Vivo Metastasis—For the induction of passive systemic anaphylaxis, BALB/c mice were sensitized by an intravenous injection of DNP-specific IgE (0.5 μg/kg). The next day, sensitized mice were challenged by an intravenous injection of DNP-HSA (250 μg/kg). To determine the effect of COX-2 on the enhanced metastatic potential of cancer cells by PSA, BALB/c mice were given an intravenous injection with scrambled (100 nM) or COX-2 siRNA (100 nM) on days 1, 5, and 7 of the time line. Three days after the injection of IgE, BALB/c mice were given an intravenous injection of B16F1 melanoma cells (2×10^5). On day 12 of the time line, lung tumor tissues were harvested. The extent of metastasis was determined as described.

In Vivo Tumorigenic Potential—To determine the effect of miR-26 on the enhanced tumorigenic potential of cancer cells by PSA, BALB/c mice were given an intravenous injection with control mimic (100 nM), miR-26a mimic (100 nM), or miR-26b mimic (100 nM) on days 0, 5, 8, 11, and 14 of the time line. Fifteen days after the injection of B16F1 cells (2×10^5), the tumorigenic potential of B16F1 cells was determined.

Chemoinvasion Assays—The invasive potential was determined by using a transwell chamber system with 8-μm pore polycarbonate filter inserts (CoSTAR, Acton, MA). The lower and upper sides of the filter were coated with gelatin and Matrigel gel, respectively. Trypsinized cells (5×10^3) in serum-free RPMI 1640 medium containing 0.1% bovine serum albumin were added to each upper chamber of the transwell. RPMI 1640 medium supplemented with 10% fetal bovine serum was placed in the lower chamber, and cells were incubated at 37 °C for 16 h. The cells were fixed with methanol, and the invaded cells were stained and counted. Results were analyzed for statistical significance using Student's *t* test. Differences were considered significant when *p* was <0.05. To examine the effect of miR-26 on the enhanced invasion potential of B16F1 melanoma cells by mast cells, lung mast cells obtained after PSA were transfected

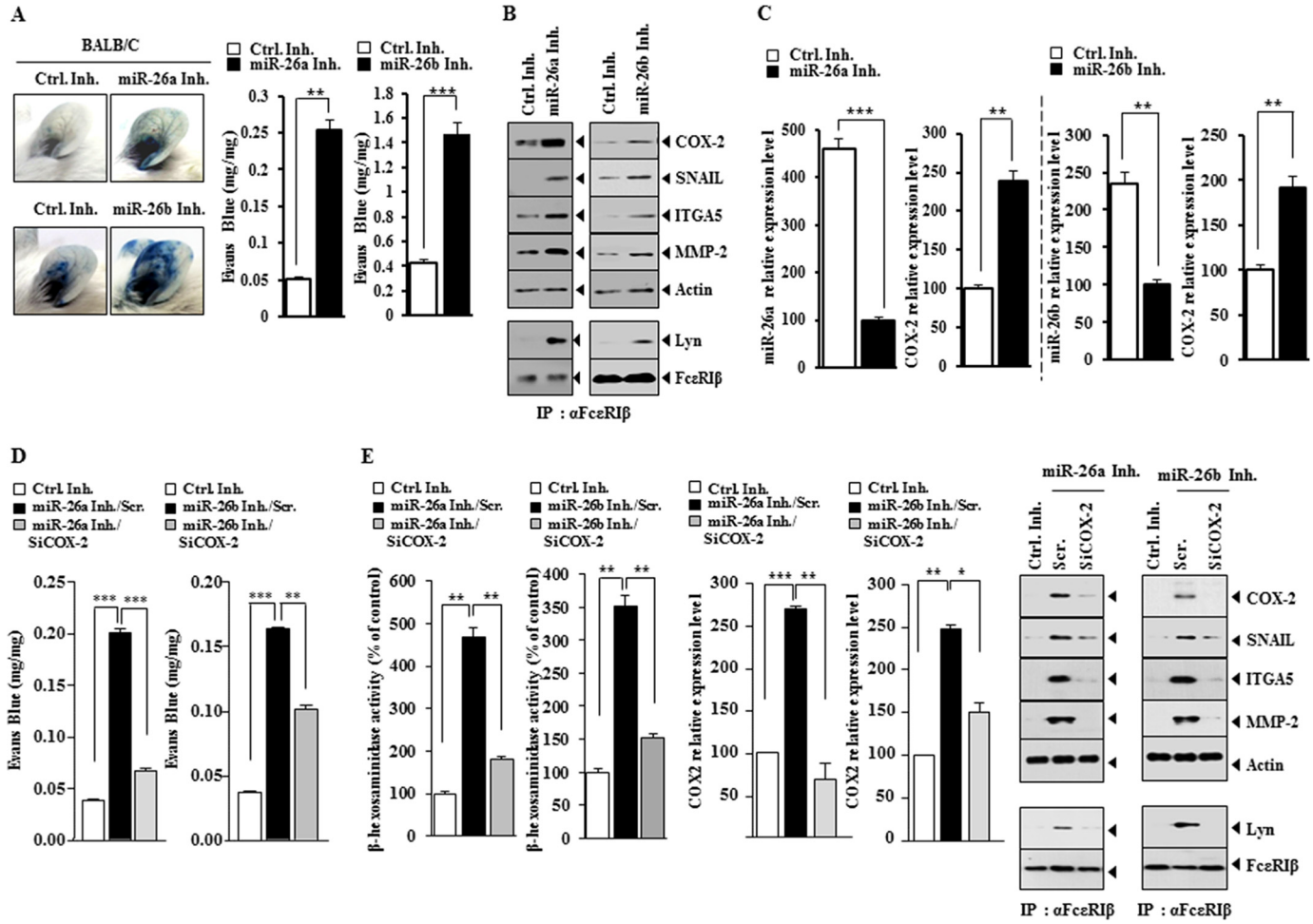

FIGURE 6. **miR-26a inhibitor and miR-26b inhibitor target COX-2 to regulate features of *in vivo* allergic inflammation.** *A*, control inhibitor (100 nM), miR-26a inhibitor (100 nM), or miR-26b inhibitor (100 nM) was injected into the ears of the indicated mice. At 8 h after injection, Evans Blue solution was injected, and the extent of vascular permeability was measured as described. Each experimental group consisted of five mice. **, $p < 0.005$; ***, $p < 0.0005$. *B*, ear lysates isolated from ear of each mouse were subjected to Western blot analysis or immunoprecipitation employing the indicated antibody, followed by Western blot analysis. *C*, ear lysate isolated was subjected to qRT-PCR analysis for determination of expression levels of miR-26a, miR-26b, or COX-2. **, $p < 0.005$; ***, $p < 0.0005$. *D*, the indicated inhibitor (100 nM) was injected along with the indicated siRNA (100 nM) into the ears of the indicated mice. At 8 h after injection, Evans Blue solution was injected, and the extent of vascular permeability was measured as described. **, $p < 0.005$; ***, $p < 0.0005$. *E*, ear lysates were subjected to Western blot analysis or immunoprecipitation employing the indicated antibody, followed by Western blot analysis. Ear lysates were also subjected to β-hexosaminidase activity assays and qRT-PCR analysis. *, $p < 0.05$; **, $p < 0.005$; ***, $p < 0.0005$. *Error bars*, S.E. *Scr.*, scrambled siRNA.

with miR-26 mimic. After transfection, conditioned medium was obtained and added to B16F1 cells for 24 h. Chemoinvasion assays were performed.

Statistical Analysis—Data were analyzed and graphed using the GraphPad Prism statistics program (GraphPad Software). Results are presented as mean ± S.E. Statistical analysis was performed using Student's *t* tests with differences between means considered significant when p was <0.05.

Results

COX-2 Is Necessary for in Vivo Allergic Inflammation—We first examined whether COX-2 would be necessary for *in vivo* allergic inflammation. TpCR in C57BL/6 mice was accompanied by increased ear thickness, but not in the COX-2(−/−) C57BL/6 mice (Fig. 1*A*). TpCR in the C57BL/6 mice was accompanied by the increased expression of COX-2, HDAC3, and TGaseII (Fig. 1*B*). HDAC3 mediates allergic inflammation by regulating the expression of MCP1 (28). TGaseII forms a feedback loop with miR-218/-181a and regulates allergic inflammation *in vitro* and *in vivo* (9). COX-2 expression is regulated by histone modifications (29). TpCR in C57BL/6 mice was accompanied by the interaction between FcεRI and Lyn and also the interaction between FcεRI and Syk (Fig. 1*B*). Ear skin mast cells isolated after the induction of TpCR in C57BL/6 mice, but not in the COX-2(−/−) C57BL/6 mice, showed the increased β-hexosaminidase activity (Fig. 1*C*). Ear skin mast cells isolated after the induction of TpCR in C57BL/6 mice showed the increased expression of COX-2, HDAC3, and TGaseII and the interaction between FcεRI and Lyn and also the interaction between FcεRI and Syk (Fig. 1*D*). PCA in the C57BL/6 mice, but not in the COX-2(−/−) C57BL/6 mice, was accompanied by increased vascular permeability (Fig. 1*E*). Western blot of ear tissue lysates showed the increased expression of COX-2, HDAC3, and TGaseII in the C57BL/6 mice by PCA, but not in the COX-2(−/−) C57BL/6 mice (Fig. 1*E*). The induction of PCA in the C57BL/6 mice was accompanied by increased β-hexosaminidase activity, but not in the COX-2(−/−) C57BL/6 mice (Fig. 1*E*). The induction of PSA was accom-

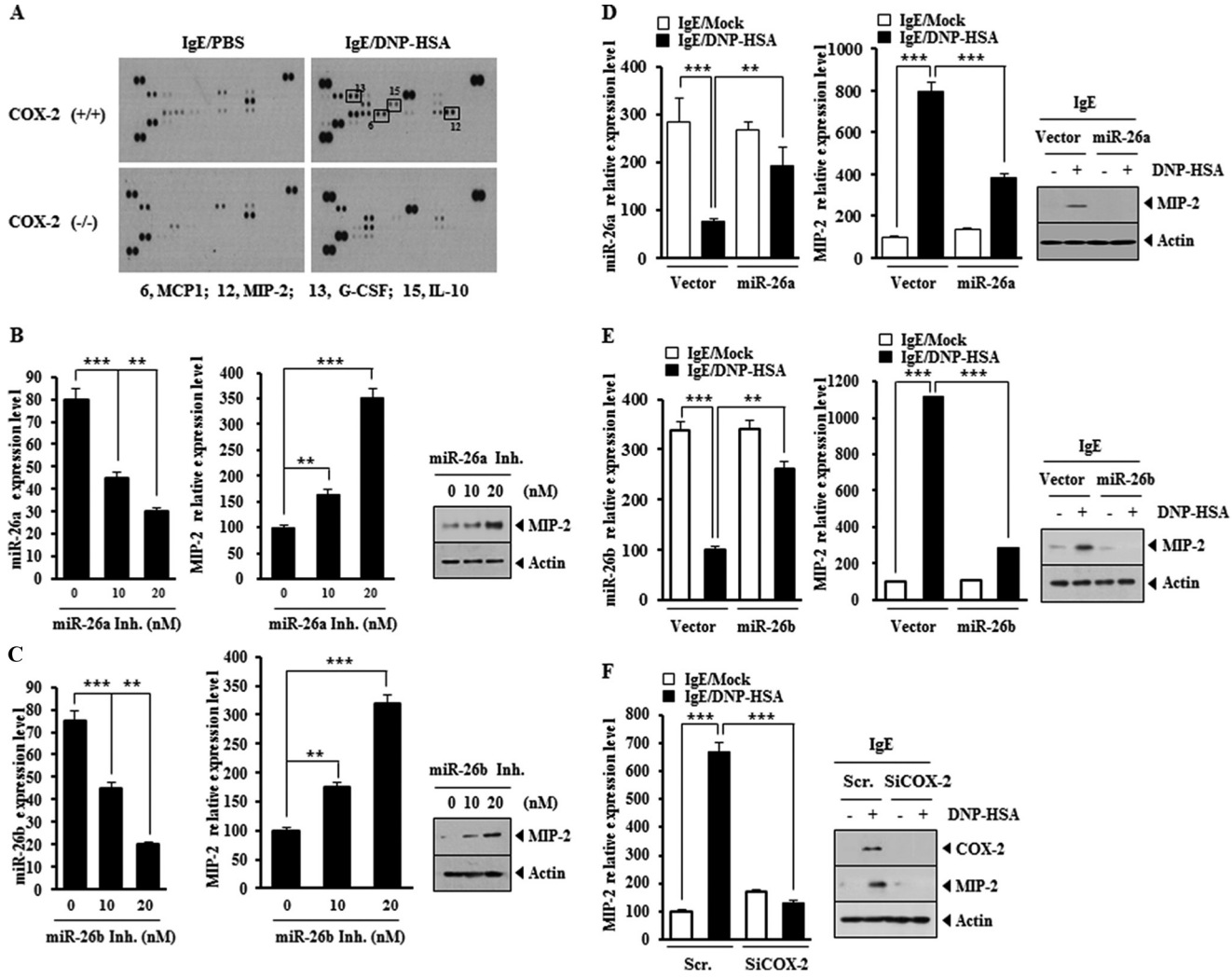

FIGURE 7. **MIP-2 is regulated by miR-26, miR-26b and COX-2.** *A*, the indicated mice were given an intravenous injection of DNP-specific IgE (0.5 μg/kg). The next day, the indicated mice were given an intravenous injection of DNP-HSA (250 μg/kg). One hour after stimulation with DNP-HSA (250 μg/kg), serum was isolated from each mouse of each experimental group of mice and subjected to cytokine array analysis. *B*, RBL2H3 cells were transfected with various concentrations of miR-26a inhibitor for 8 h. Cell lysates were subjected to qRT-PCR analysis (*left*). **, $p < 0.005$; ***, $p < 0.0005$. Cell lysates were also subjected to Western blot analysis (*right*). *C*, same as *B* except that RBL2H3 cells were transfected with miR-26b inhibitor. **, $p < 0.005$; ***, $p < 0.0005$. *D*, RBL2H3 cells were transfected with the indicated construct (each at 1 μg) prior to sensitization with DNP-specific IgE (100 ng/ml). The IgE-sensitized RBL2H3 cells were then stimulated with DNP-HSA (100 ng/ml) for 1 h. Cell lysates were subjected to qRT-PCR analysis (*left*) and Western blot analysis (*right*). **, $p < 0.005$; ***, $p < 0.0005$. *E*, same as *D* except that RBL2H3 cells were transfected with miR-26b construct (1 μg). **, $p < 0.005$; ***, $p < 0.0005$. *F*, RBL2H3 cells were transfected with the indicated siRNA (10 nM each) prior to sensitization with DNP-specific IgE (100 ng/ml). The IgE-sensitized RBL2H3 cells were then stimulated with DNP-HSA (100 ng/ml) for 1 h. Cell lysates were subjected to qRT-PCR analysis (*left*) and Western blot analysis (*right*). ***, $p < 0.0005$. *Error bars*, S.E. *Scr.*, scrambled siRNA.

panied by an increased expression of COX-2 (Fig. 1*F*). These results suggest that COX-2 is necessary for *in vivo* allergic inflammation.

The Down-regulation of COX-2 Negatively Regulates Allergic Inflammation in Vitro and in Vivo—We further examined the role of COX-2 in allergic inflammation. The down-regulation of COX-2 by siCOX-2 prevented antigen from increasing the expression of HDAC3 and TGaseII in antigen-stimulated RBL2H3 cells (Fig. 2*A*) and prevented antigen from increasing β-hexosaminidase activity in antigen-stimulated RBL2H3 cells (Fig. 2*B*). We examined the effect of COX-2 on PSA. The *in vivo* down-regulation of COX-2 prevented the antigen from decreasing the rectal temperature of the mice (Fig. 2*C*). The *in vivo* down-regulation of COX-2 prevented antigen from increasing the expression levels of HDAC3 and MIP-2 and prevented antigen from inducing an interaction between FcϵRI and Lyn (Fig. 2*D*). The role of MIP-2, a macrophage inhibitory protein-2, in allergic atopic dermatitis has been reported (31). The down-regulation of COX-2 occurred at the transcriptional level by COX-2 siRNA and prevented antigen-induced increase in β-hexosaminidase activity in the mouse model of PSA (Fig. 2*D*). The *in vivo* down-regulation of COX-2 negatively regulated vascular permeability, β-hexosaminidase activity, the expression of HDAC3 and MIP-2, and the interaction between FcϵRI and Lyn in the mouse model of PCA (Fig. 2*E*). These results indicate that COX-2 is necessary for allergic inflammation *in vitro* and *in vivo*.

miR-26a and miR-26b Target COX-2—miRNAs are known to regulate allergic inflammation (9, 10). TargetScan analysis predicted the binding of miR-26a and miR-26b to the 3′-UTR of

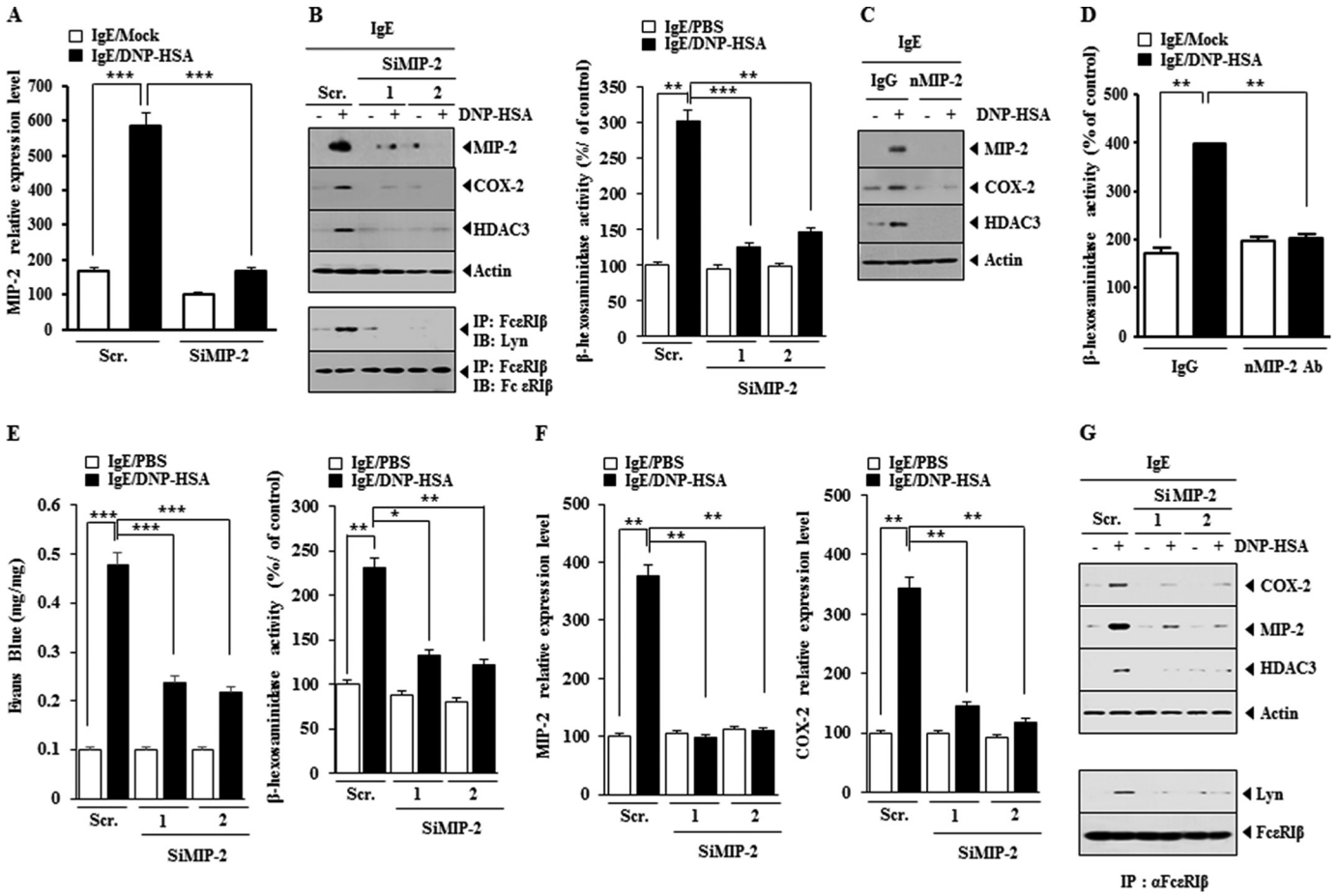

FIGURE 8. **MIP-2 regulates *in vitro* allergic inflammation.** *A*, RBL2H3 cells were transfected with the indicated siRNA (10 nM each) prior to sensitization with DNP-specific IgE (100 ng/ml). The IgE-sensitized RBL2H3 cells were then stimulated with DNP-HSA (100 ng/ml) for 1 h. Cell lysates were subjected to qRT-PCR analysis. *, $p < 0.05$; **, $p < 0.005$; ***, $p < 0.0005$. *B*, same as *A* except that Western blot, immunoprecipitation, and β-hexosaminidase activity assays were performed. **, $p < 0.005$; ***, $p < 0.0005$. *C*, the IgE-sensitized RBL2H3 cells were preincubated with neutralizing nMCP1 antibody (10 μg/ml) or isotype-matched IgG (10 μg/ml) for 2 h, followed by stimulation with DNP-HSA (100 ng/ml) for 2 h. Cell lysates were subjected to Western blot analysis. *D*, same as *C* except that β-hexosaminidase activity assays were performed. **, $p < 0.005$. *E*, BALB/c mice were given an intradermal injection of DNP-specific IgE (0.5 μg/kg). The next day, BALB/c mice were given an intravenous injection of scrambled (*Scr.*) (100 nM) or MIP-2 siRNA (100 nM). One hour after the injection of siRNA, BALB/c mice were given an intravenous injection of PBS or DNP-HSA (250 μg/kg) along with 2% (v/v) Evans Blue solution. One hour after the injection of Evans Blue solution, the dye was eluted from the ear in 700 μl of formamide at 63 °C. The absorbance was measured at 620 nm. Ear tissue lysates were isolated and subjected to β-hexosaminidase activity assays. *, $p < 0.05$; **, $p < 0.005$; ***, $p < 0.0005$. *F*, ear tissue lysates were subjected to qRT-PCR to determine the expression of MIP-2 mRNA and COX-2 mRNA. **, $p < 0.005$. *G*, ear tissue lysate were subjected to Western blot analysis (*top*) or immunoprecipitated with the indicated antibody, followed by Western blot analysis (*bottom*). *Error bars*, S.E.

COX-2 (Fig. 3*A*). Antigen stimulation in RBL2H3 decreased the expression of miR-26a and miR-26b (Fig. 3*B*). The overexpression of miR-26a (Fig. 3*C*) or miR-26b (Fig. 3*D*) decreased luciferase activity associated with the wild type 3′-UTR of COX-2, but not mutant 3′-UTR of COX-2, in antigen-stimulated RBL2H3 cells. The down-regulation of COX-2 did not affect the expression of miR-26a or miR-26b (data not shown), suggesting that miR-26a/-26b act upstream of COX-2. These results suggest that miR-26 and miR-26b target the expression of COX-2 to regulate allergic inflammation.

miR-26a and miR-26b Negatively Regulate the in Vitro Allergic Inflammation—The overexpression of miR-26a construct and miR-26b construct prevented antigen-induced increase in β-hexosaminidase activity (Fig. 4*A*) and prevented antigen from increasing the expression of HDAC3, COX-2, MCP1, and TGaseII in RBL2H3 cells (Fig. 4*B*). The overexpression of miR-26a and miR-26b prevented antigen from inducing an interaction between FcεRI and Lyn (Fig. 4*B*) and prevented antigen from increasing the levels of ROS and active Rac1 in RBL2H3 cells (Fig. 4*C*). miR-26a mimic and miR-26b mimic prevented antigen from increasing the expression of COX-2 and HDAC3 and prevented antigen from inducing an interaction between FcεRI and Lyn in RBL2H3 cells (Fig. 4*D*). miR-26a mimic and miR-26b mimic prevented antigen-induced increase in β-hexosaminidase activity in RBL2H3 cells (Fig. 4*E*). These results suggest that miR-26a and miR-26b negatively regulate the features of *in vitro* allergic inflammation.

miR-26 Inhibitors Target COX-2 to Regulate in Vitro Allergic Inflammation in an IgE-independent Manner—Because overexpression of miR-26a and miR-26b negatively regulated allergic inflammation, we examined the effect of miR-26 down-regulation on the allergic inflammation. miR-26a inhibitor and miR-26 inhibitor increased the expression of COX-2 mRNA (Figs. 5, *A* and *E*) and COX-2 protein (Figs. 5, *B* and *F*). miR-26a inhibitor and miR-26b inhibitor increased the expression of hallmarks of allergic inflammation, such as MMP-2, SNAIL,

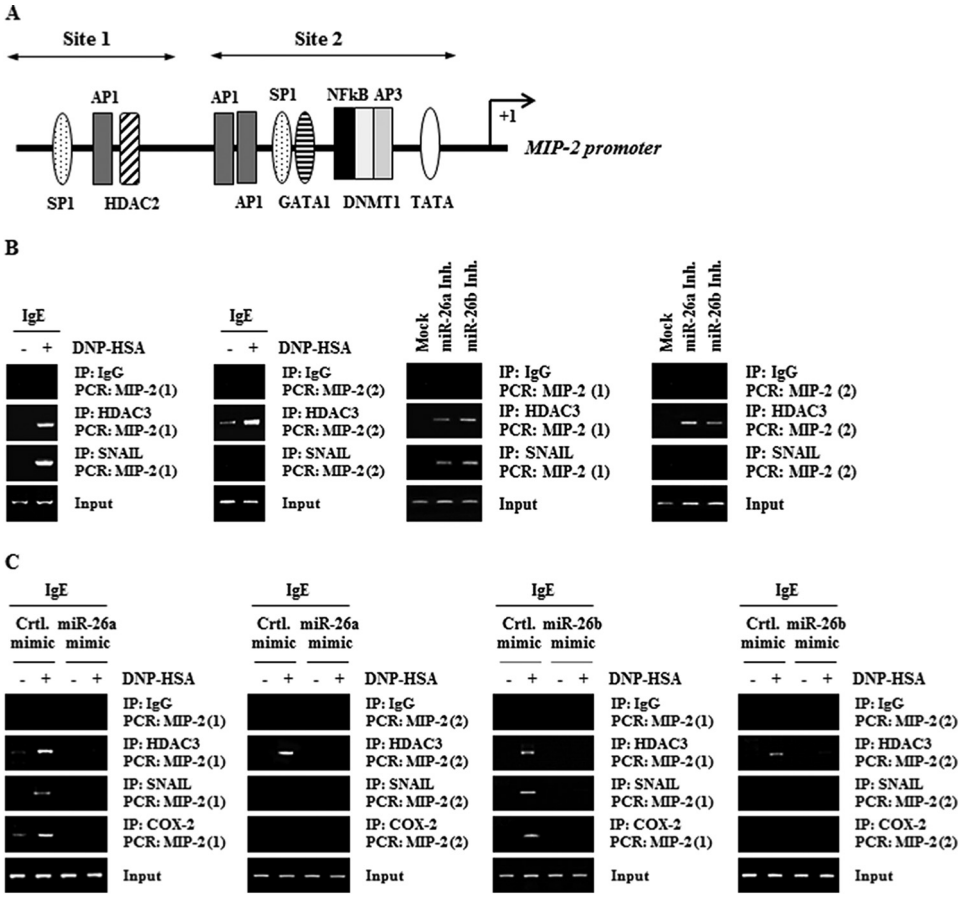

FIGURE 9. **The expression regulation of MIP-2.** *A*, potential binding sites of transcriptional factors in the promoter sequences of MIP-2. *B*, the IgE-sensitized RBL2H3 cells were stimulated with DNP-HSA (100 ng/ml) for 1 h. Cell lysates were subjected to ChIP assays employing the indicated antibody. RBL2H3 cells were transfected with control inhibitor (10 nM), miR-26a inhibitor (10 nM), or miR-26b inhibitor (10 nM). At 48 h after transfection, cell lysates were subjected to ChIP assays. *C*, RBL2H3 cells were transfected with the indicated mimic (10 nM each) prior to sensitization with DNP-specific IgE (100 ng/ml). The IgE-sensitized RBL2H3 cells were then stimulated with DNP-HSA (100 ng/ml) for 1 h. Cell lysates were subjected to ChIP assays. *IP*, immunoprecipitation.

integrin α_5 (ITGA5), and COX-2 (Fig. 5, *C* and *G*). miR-26a inhibitor and miR-26b inhibitor increased β-hexosaminidase activity in RBL2H3 cells (Fig. 5, *C* and *G*). The down-regulation of COX-2 prevented miR-26b inhibitors from increasing the expression of hallmarks of allergic inflammation and β-hexosaminidase activity (Fig. 5, *D* and *H*). These results suggest that miR-26 inhibitors target COX-2 to regulate *in vitro* allergic inflammation.

miR-26 Inhibitors Induce Features of in Vivo Allergic Inflammation by Targeting COX-2—We examined the effect of miR-26 inhibitors on *in vivo* allergic inflammation. The injection of miR-26a inhibitor or miR-26b inhibitor into the ears of BALB/c mice increased vascular permeability (Fig. 6*A*). miR-26a inhibitor and miR-26b inhibitor increased the expression of hallmarks of allergic inflammation, such as MMP-2, SNAIL, integrin α_5, and COX-2, and induced an interaction between FcϵRI and Lyn in BALB/c mice (Fig. 6*B*). miR-26a inhibitor and miR-26b inhibitor increased the expression of COX-2 mRNA (Fig. 6*C*). The down-regulation of COX-2 prevented miR-26 inhibitors from increasing vascular permeability (Fig. 6*D*). The down-regulation of COX-2 inhibited effects of miR-26 inhibitors on the expression of hallmarks of allergic inflammation, an interaction between FcϵRI and Lyn, and β-hexosaminidase activity (Fig. 6*E*). These results suggest that miR-26a inhibitor and miR-26b inhibitor induce features of *in vivo* allergic inflammation by targeting COX-2.

MIP-2 Is Regulated by miR-26a/-26b and COX-2—Cytokine array analysis was performed to better understand the mechanisms associated with COX-2-mediated allergic inflammation. Serum of the COX-2(+/+) or COX-2(−/−) mouse was isolated after the induction of PSA. PSA induced the expression of various cytokines, such as MIP-2, MCP1, IL-10, and G-CSF, in a COX-2-dependent manner (Fig. 7*A*). The expression of MIP-2 is significantly elevated in ovalbumin-dependent mouse model of asthma (30). In allergic airway inflammation, the expression of MIP-2 is increased (31). miR-26a inhibitor and miR-26b inhibitor increased the expression of MIP-2 in RBL2H3 cells in a dose-dependent manner (Fig. 7, *B* and *C*). The overexpression of miR-26a and miR-26b prevented antigen form increasing the expression of MIP-2 in RBL2H3 cells (Fig. 7, *D* and *E*). The down-regulation of COX-2 prevented antigen from increasing the expression of MIP-2 in RBL2H3 cells (Fig. 7*F*). These results suggest that the expression of MIP-2 is regulated by miR-26a/-26b and COX-2. It will be interesting to examine the effect of COX-2 on the expression of IL-10 and G-CSF.

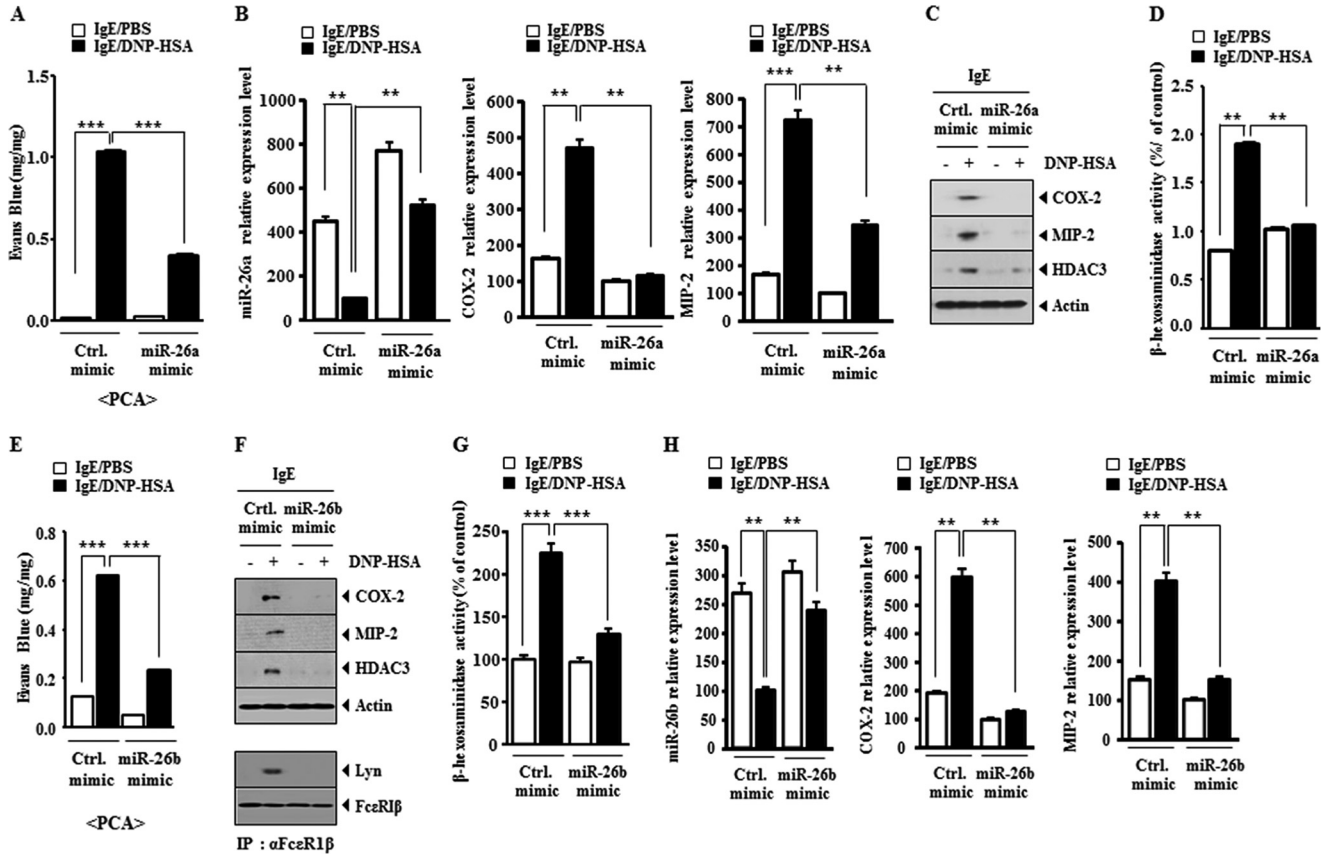

FIGURE 10. **miR-26a mimic and miR-26b mimic negatively regulate passive cutaneous anaphylaxis.** *A*, BALB/c mice were given an intradermal injection of DNP-specific IgE antibody (0.5 μg/kg) along with an intravenous injection of control mimic (100 nM) or miR-26a mimic (100 nM). The next day, BALB/C mice were given an intravenous injection of PBS or DNP-HSA (250 μg/kg) along with 2% (v/v) Evans Blue solution. One hour after the injection, the extent of vascular permeability was determined as described. Means ± S.E. (*error bars*) of three independent experiments are depicted. Each experimental group consisted of five mice. ***, $p < 0.0005$. *B*, ear tissue lysates were subjected to qRT-PCR analysis to determine the expression of miR-26a, COX-2, and MIP-2. **, $p < 0.005$; ***, $p < 0.0005$. *C*, ear tissue lysates were subjected to Western blot analysis. *D*, same as *C* except that β-hexosaminidase activity assays were performed. **, $p < 0.005$. *E*, BALB/c mice were given an intradermal injection of DNP-specific IgE antibody (0.5 μg/kg) along with an intravenous injection of control mimic (100 nM) or miR-26b mimic (100 nM). The next day, BALB/c mice were given an intravenous injection of PBS or DNP-HSA (250 μg/kg) along with 2% (v/v) Evans Blue solution. One hour after the injection, the extent of vascular permeability was determined as described. Means ± S.E. of three independent experiments are depicted. Each experimental group consisted of five mice. ***, $p < 0.0005$. *F*, ear tissue lysates were subjected to Western blot analysis (*top*). Ear tissue lysates were also subjected to immunoprecipitation (*IP*), followed by Western blot analysis (*bottom*). *G*, same as *F* except that β-hexosaminidase activity assays were performed. ***, $p < 0.0005$. *H*, ear tissue lysates were subjected to qRT-PCR analysis to determine the expression of miR-26b, MIP-2, and COX-2. **, $p < 0.005$.

MIP-2 Regulates the in Vitro and in Vivo Allergic Inflammation—We examined the role of MIP-2 in allergic inflammation. The down-regulation of MIP-2 in antigen-stimulated RBL2H3 cells (Fig. 8*A*) prevented antigen-induced increase in the expression of HDAC3 and COX-2 and prevented antigen-induced interaction between FcεRI and Lyn (Fig. 8*B*). Furthermore, the down-regulation of MIP-2 prevented antigen from increasing β-hexosaminidase activity (Fig. 8*B*). The neutralizing MIP-2 antibody prevented antigen-induced increased expression of HDAC3 and COX-2 (Fig. 8*C*) and prevented antigen-induced increase in β-hexosaminidase activity (Fig. 8*D*). The down-regulation of MIP-2 exerted a negative effect on PCA and prevented antigen-induced β-hexosaminidase activity (Fig. 8*E*) and antigen-induced increase in COX-2 expression at the transcriptional level (Fig. 8*F*). The down-regulation of MIP-2 prevented antigen from increasing the expression of HDAC3 and COX-2 and also prevented antigen from inducing an interaction between FcεRI and Lyn in a mouse model of PCA (Fig. 8*G*). These results suggest that MIP-2 regulates *in vitro* and *in vivo* allergic inflammation.

The Expression Regulation of MIP-2—We wanted to investigate the molecular mechanisms associated with the increased expression of MIP-2 during allergic inflammation. MIP-2 promoter sequences contain the binding sites for various transcription factors, such as SP1, AP1, YY1, SNAIL, and NF-κB (Fig. 9*A*). ChIP assays showed the binding of HDAC3 and SNAIL to the promoter sequences of MIP-2 in antigen-stimulated RBL2H3 cells (Fig. 9*B*). miR-26a inhibitor and miR-26b inhibitor induced the binding of HDAC3 and SNAIL to the promoter sequences of MIP-2 (Fig. 9*B*). miR-26a mimic and miR-26b mimic prevented antigen from inducing the binding of HDAC3, SNAIL, and COX-2 to the promoter sequences of MIP-2 (Fig. 9*C*). COX-2 does not bind to the promoter sequences of miR-26a or miR-26b,[4] suggesting that COX-2 acts downstream of miR-26a/-26b. These results confirm that the expression of MIP-2 is regulated by the miR-26a/-26b-COX-2 axis.

[4] Y. Kwon, Y. Kim, S. Eom, M. Kim, D. Park, H. Kim, K. Noh, H. Lee, Y. S. Lee, J. Choe, Y. M. Kim, and D. Jeoung, unpublished observations.

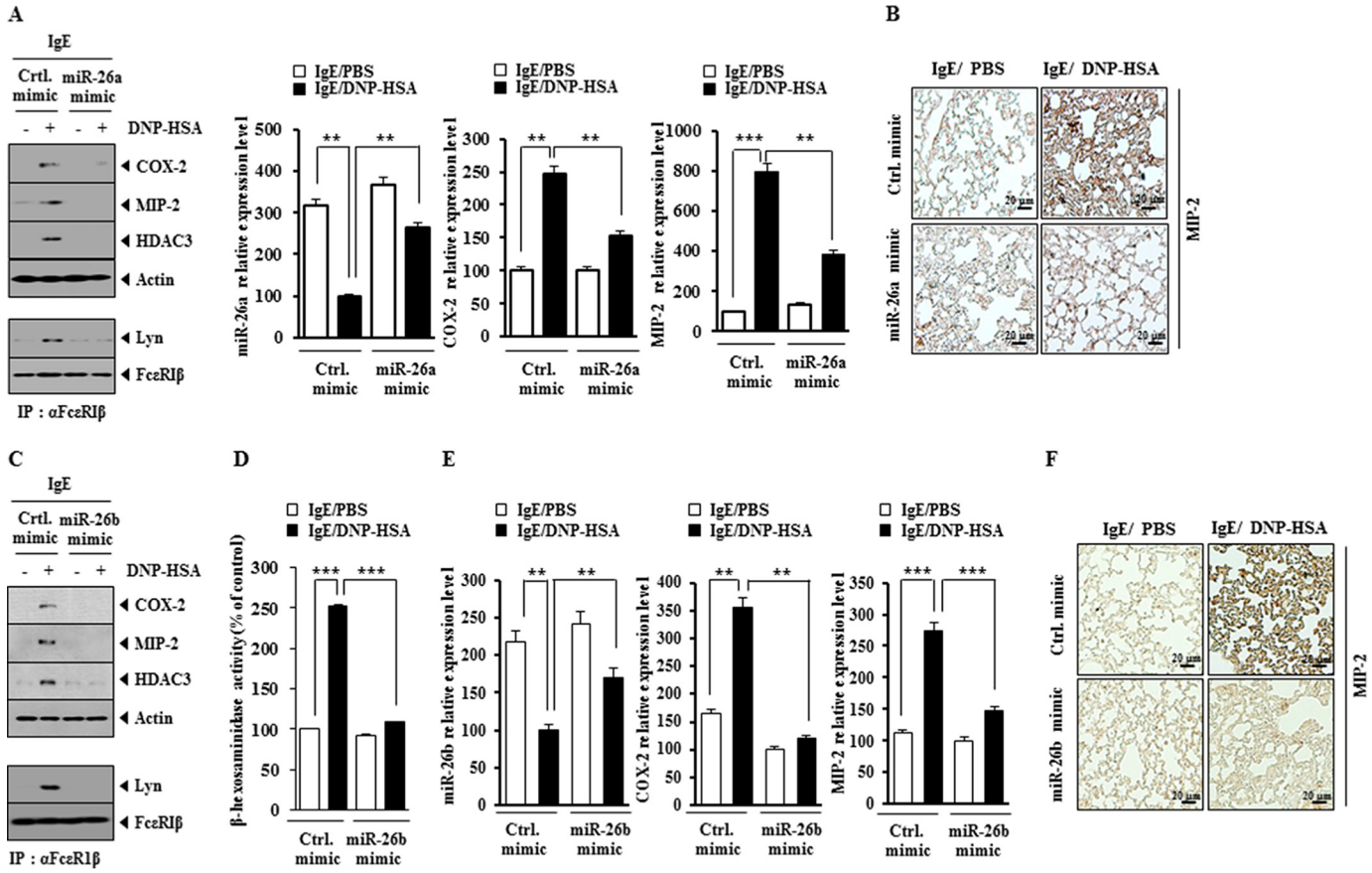

FIGURE 11. **miR-26a mimic and miR-26b mimic negatively regulate passive systemic anaphylaxis.** *A*, BALB/c mice were given intravenous injection of DNP-specific IgE (0.5 μg/kg) along with control mimic (100 nM) or miR-26a mimic (100 nM). The next day, BALB/c mice were given an intravenous injection of DNP-HSA (250 μg/kg). One hour after stimulation with DNP-HSA (250 μg/kg), lung tissue lysates were isolated from each mouse of each experimental group and were subjected to Western blot analysis or immunoprecipitated (*IP*) with the indicated antibody, followed by Western blot analysis. Lung tissue lysates were also subjected to qRT-PCR analysis to determine the expression of miR-26a and COX-2. **, $p < 0.005$; ***, $p < 0.0005$. *B*, immunohistochemistry staining employing lung tissue was performed as described. *C*, BALB/c mice were given intravenous injection of DNP-specific IgE (0.5 μg/kg) along with control mimic (100 nM) or miR-26b mimic (100 nM). The next day, BALB/c mice were given an intravenous injection of DNP-HSA (250 μg/kg). One hour after stimulation with DNP-HSA (250 μg/kg), lung tissue lysates were isolated from each mouse of each experimental group and were subjected to Western blot analysis (*top*) or immunoprecipitated with the indicated antibody, followed by Western blot analysis (*bottom*). *D*, lung tissue lysates were subjected to β-hexosaminidase activity assays. ***, $p < 0.0005$. *E*, lung tissue lysates were subjected to qRT-PCR to determine the expression level of miR-26b, MIP-2, and COX-2. **, $p < 0.005$; ***, $p < 0.0005$. *F*, immunohistochemistry staining employing anti-MIP-2 antibody was performed as described. *Error bars*, S.E.

miR-26a Mimic and miR-26b Mimic Negatively Regulate the Passive Cutaneous Anaphylaxis—We examined the effect of miR-26a and miR-26b on the *in vivo* allergic inflammation. miR-26a mimic and miR-26b mimic exerted negative effects on the increased vascular permeability by PCA (Figs. 10, *A* and *E*). qRT-PCR analysis showed that miR-26a mimic and miR-26b mimic prevented antigen-induced increase in COX-2 mRNA and MIP-2 mRNA expression by PCA (Fig. 10, *B* and *H*). miR-26a and miR-26b mimic exerted negative effects on the increased expression of COX-2, HDAC3, and MIP-2 by PCA (Fig. 10, *C* and *F*). miR-26a mimic and miR-26b mimic also exerted negative effects on the increased β-hexosaminidase activity by PCA (Fig. 10, *D* and *G*). miR-26b mimic negatively regulated an interaction between FcεRI and Lyn induced by PCA (Fig. 10*F*). These results suggest that the overexpression of miR-26a and miR-26b negatively regulates PCA.

miR-26a Mimic and miR-26b Mimic Negatively Regulate Passive Systemic Anaphylaxis—Because miR-26a mimic and miR-26b mimic negatively regulated PCA, we examined the effect of miR-26a mimic and miR-26b mimic on PSA. miR-26a mimic and miR-26b mimic prevented antigen-induced increase in the expression of HDAC3, COX-2, and MIP-2 and also prevented DNP-HSA from inducing an interaction between FcεRI and Lyn in a mouse model of PSA (Fig. 11, *A* and *C*). miR-26a mimic and miR-26b mimic prevented DNP-HAS-induced increase in COX-2 and MIP-2 expression at the transcriptional level (Fig. 11, *A* and *E*). Immunohistochemistry staining showed that miR-26a mimic and miR-26b mimic prevented DNP-HSA from increasing the expression of MIP-2 in a mouse model of PSA (Fig. 11, *B* and *F*). In addition, miR-26b mimic prevented DNP-HSA from increasing β-hexosaminidase activity (Fig. 11*D*). These results suggest that miR-26a mimic and miR-26b mimic negatively regulate PSA.

miR-26a Mimic and miR-26b Mimic Negatively Regulate Allergic Inflammation-promoted Enhanced Tumorigenic Potential—PSA enhances the tumorigenic potential of cancer cells (9, 10). PSA enhanced the tumorigenic potential of mouse melanoma B16F1 cells less than malignant melanoma cells (Figs. 12*A* and 13*A*). miR-26a mimic and miR-26b mimic exerted negative effects on the enhanced tumorigenic potential

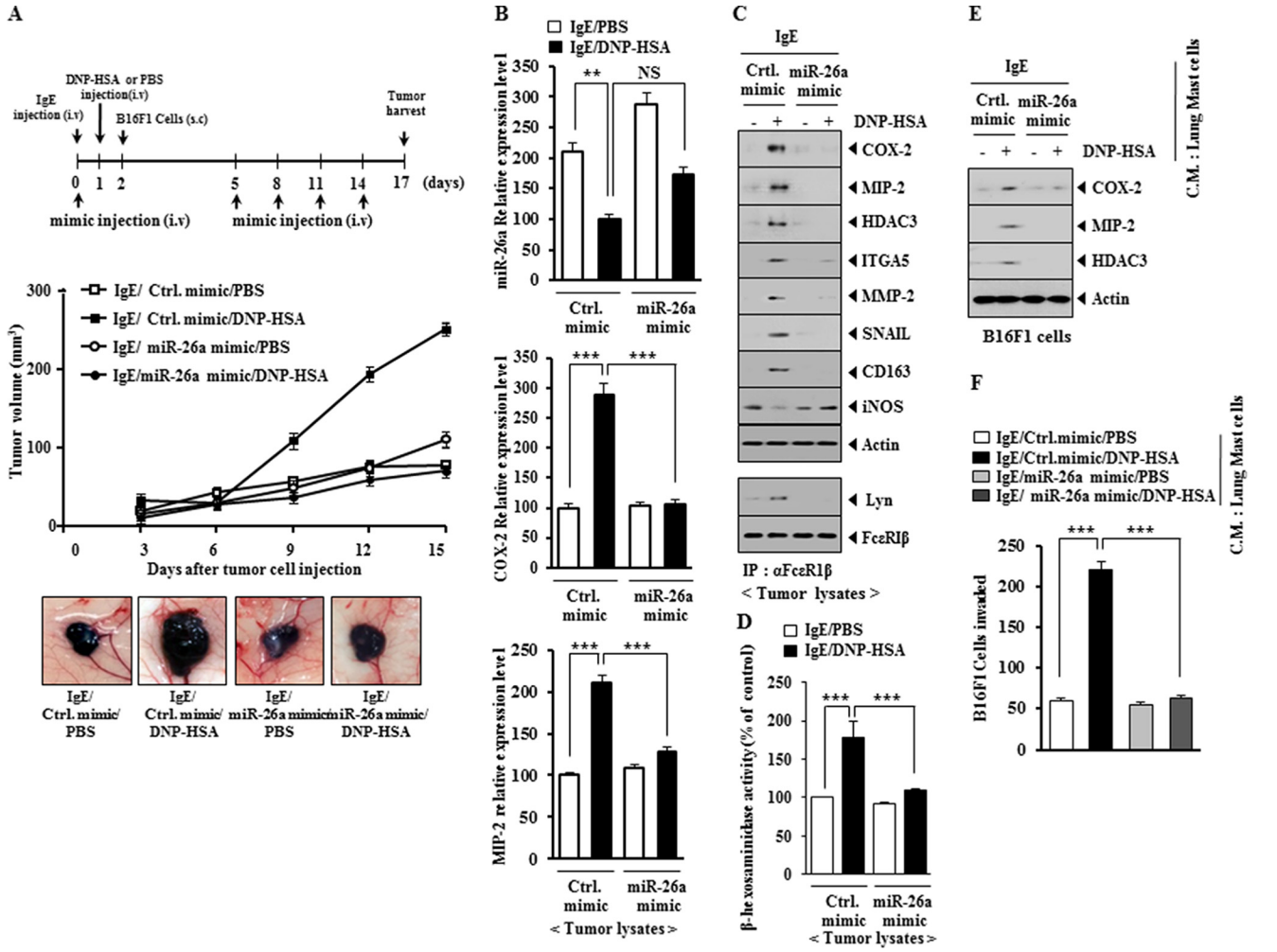

FIGURE 12. **miR-26a mimic negatively regulates PSA-promoted enhanced tumorigenic potential of B16F1 melanoma cells.** *A*, BALB/c mice were sensitized to DNP-specific IgE (0.5 μg/kg) by an intravenous (*i.v.*) injection. The next day, BALB/c mice were given an intravenous injection of DNP-HSA (250 μg/kg). Each mouse received an injection of B16F1 melanoma cells (2×10^5) on day 2 of the time line. BALB/c mice were given an intravenous injection with control mimic (100 nM) or miR-26a mimic (100 nM) on days 0, 5, 8, 11, and 14 of the time line. Fifteen days after the injection of B16F1 cells, the tumorigenic potential of B16F1 cells was determined. *B*, qRT-PCR analysis employing tumor tissue lysates was performed to determine the expression of miR-26a, COX-2, and MIP-2. **, $p < 0.005$; ***, $p < 0.0005$. *NS*, not significant. *C*, tumor tissue lysates from each experimental group were subjected to Western blot analysis and were also subjected to immunoprecipitation (*IP*) (2 μg/ml), followed by Western blot analysis. *D*, tumor tissue lysates were subjected to β-hexosaminidase activity assays. ***, $p < 0.0005$. *E*, the conditioned medium of lung mast cells after PSA induction was added to B16F1 cells for 24 h. Cell lysates were subjected to Western blot analysis. *F*, the conditioned medium of lung mast cells after PSA induction was added to B16F1 melanoma cells. An invasion assay was performed as described. ***, $p < 0.0005$. *Error bars*, S.E.

of B16F1 cells by PSA (Figs. 12*A* and 13*A*). qRT-PCR employing tumor tissue lysates showed that miR-26a mimic and miR-26b mimic negatively regulated the expression of COX-2 and MIP-2 (Figs. 12*B* and 13*B*). miR-26a mimic and miR-26b mimic prevented antigen-induced increased expression of HDAC3, COX-2, MMP-2, SNAIL, integrin α_5, and MIP-2 and also prevented antigen from regulating the expression of CD163 and iNOS (Figs. 12*C* and 13*C*). CD163 is a marker of the activated macrophages, whereas iNOS is a marker of the inhibitory macrophages (9). This suggests that allergic inflammation activates macrophages, which in turn may enhance the tumorigenic potential of cancer cells. In other words, allergic inflammation may involve the interaction between mast cells and macrophages and the interaction between cancer cells and stromal cells, such as mast cells and macrophages. miR-26a mimic and miR-26b mimic prevented an interaction between FcεRI and Lyn (Figs. 12*C* and 13*C*). Allergic inflammation-promoted enhanced tumorigenic potential involved increased β-hexosaminidase activity (Figs. 12*D* and 13*D*). miR-26a mimic and miR-26b mimic exerted negative effects on the increased β-hexosaminidase activity by PSA (Figs. 12*D* and 13*D*). The conditioned medium of lung mast cells obtained after the induction of PSA increased the expression of HDAC3, COX-2, and MIP-2 in B16F1 cells (Figs. 12*E* and 13*E*). The fact that B16F1 cells showed increased expression of MIP-2 suggests that there is a positive feedback relationship between mast cells and cancer cells. miR-26a mimic and miR-26b mimic exerted negative effects on the increased expression of HDAC3, COX-2, and MIP-2 in B16F1 cells by the conditioned medium of lung mast cells (Figs. 12*E* and 13*E*). miR-26a mimic and miR-26b mimic negatively regulated the enhanced invasion potential of B16F1 cells by PSA-activated lung mast cells (Figs. 12*F* and 13*F*). These results suggest that miR-26a mimic and miR-26b mimic negatively regulate allergic inflammation-promoted

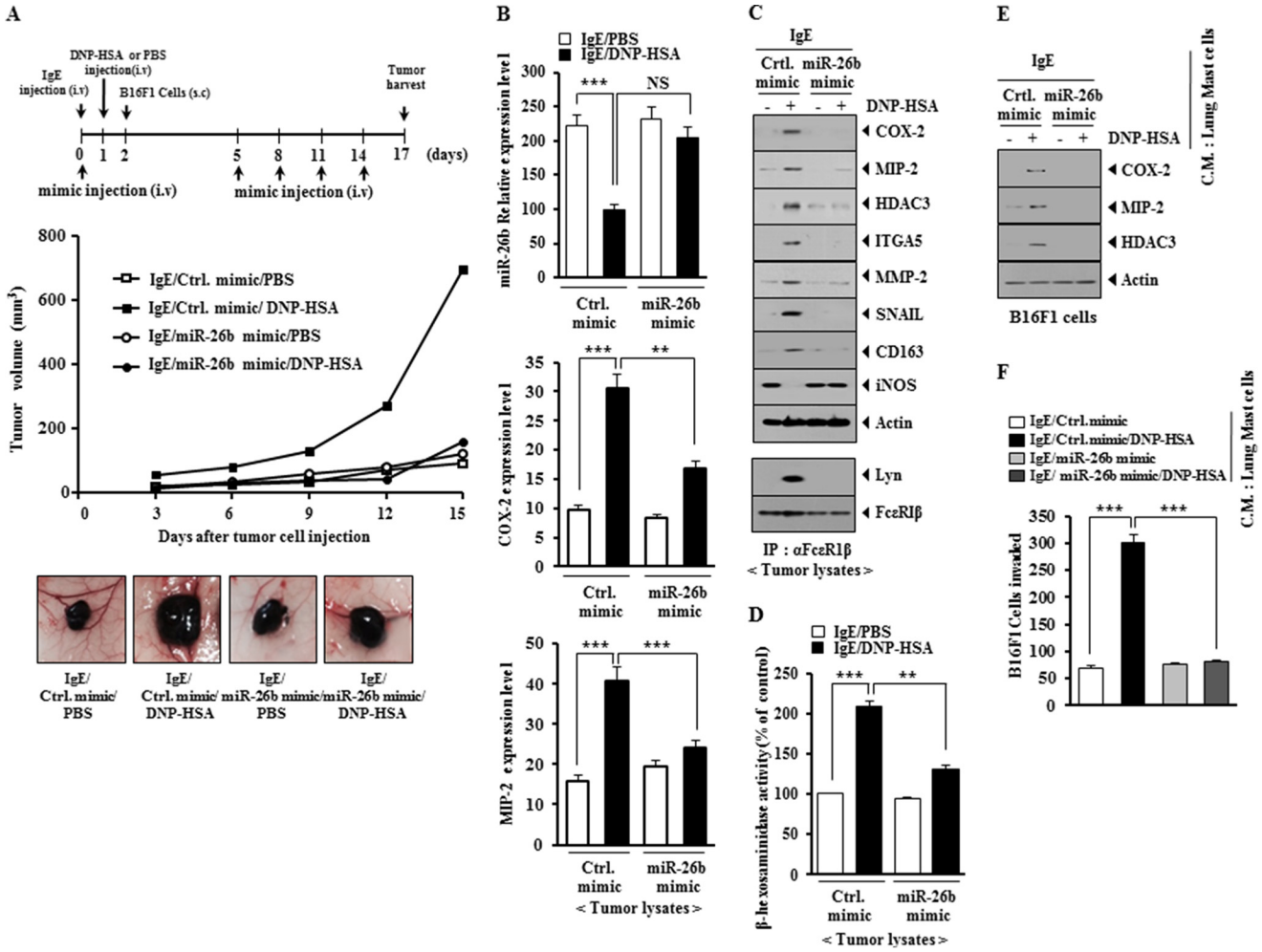

FIGURE 13. **miR-26b mimic negatively regulates PSA-promoted enhanced tumorigenic potential of B16F1 melanoma cells.** *A*, BALB/c mice were sensitized to DNP-specific IgE (0.5 μg/kg) by an intravenous (*i.v.*) injection. The next day, BALB/c mice were given an intravenous injection of DNP-HSA (250 μg/kg). Each mouse received an injection of B16F1 melanoma cells (subcutaneously; *s.c.*) (2×10^5) on day 2 of the time line. BALB/c mice were given an intravenous injection with control mimic (100 nM) or miR-26b mimic (100 nM) on days 0, 5, 8, 11, and 14 of the time line. Fifteen days after the injection of B16F1 cells, the tumorigenic potential of B16F1 cells was determined. *B*, qRT-PCR analysis employing tumor tissue lysates was performed to determine the expression of miR-26b, COX-2, and MIP-2. **, $p < 0.005$; ***, $p < 0.0005$. *C*, tumor tissue lysates from each experimental group were subjected to Western blot analysis and were also subjected to immunoprecipitation (2 μg/ml), followed by Western blot analysis. *D*, tumor tissue lysates were subjected to β-hexosaminidase activity assays. **, $p < 0.005$; ***, $p < 0.0005$. *E*, the conditioned medium of lung mast cells after PSA induction was added to B16F1 melanoma cells for 24 h. Cell lysates were subjected to Western blot analysis. *F*, the conditioned medium of lung mast cells after PSA induction was added to B16F1 cells. An invasion assay was performed as described. ***, $p < 0.0005$. *Error bars*, S.E.

enhanced tumorigenic potential by exerting negative effects on the positive feedback between mast cells and cancer cells mediated by MIP-2.

miR-26 Negatively Regulates the Interaction between Mast Cells and Macrophages during Allergic Inflammation—We previously reported a positive feedback loop between mast cells and macrophages during allergic inflammation (10). We examined the effect of miR-26a mimic and miR-26b mimic on the positive feedback relationship between mast cells and macrophages during allergic inflammation (Fig. 14*A*). miR-26a mimic and miR-26b mimic prevented antigen from increasing the expression of HDAC3 and COX-2 and prevented antigen-induced interaction between FcεRI and Lyn in a mouse model of PSA (Fig. 14*B*). miR-26a mimic and miR-26b mimic decreased the expression of miR-26a and miR-26b, respectively (Fig. 14*C*). miR-26a mimic and miR-26b mimic prevented the conditioned medium of lung mast cells, obtained after PSA, from regulating the expression of CD163 and iNOS in lung macrophages (Fig. 14*D*). The *in vivo* down-regulation of COX-2 prevented antigen-induced increased expression of MIP-2 and regulation of the expression of CD163 and iNOS in lung macrophages in the mouse model of PSA (Fig. 14*E*). The addition of conditioned medium of lung macrophages obtained after PSA to lung mast cells increased β-hexosaminidase activity and MIP-2 and HDAC3 expression and induced an interaction between FcεRI and Lyn in a COX-2-dependent manner (Fig. 14*F*). These results suggest that macrophages, activated during allergic inflammation, activate mast cells in a COX-2-dependent manner. These results suggest that the miR-26a mimic and miR-26b mimic negatively the regulate positive feedback relationship between mast cells and macrophages during allergic inflammation.

miR-26a Mimic and miR-26b Mimic Negatively Regulate the Angiogenic Potential of Mast Cells—Allergic inflammation-promoted enhanced tumorigenic potential is accompanied by an enhanced angiogenic potential (9). COX-2 is necessary

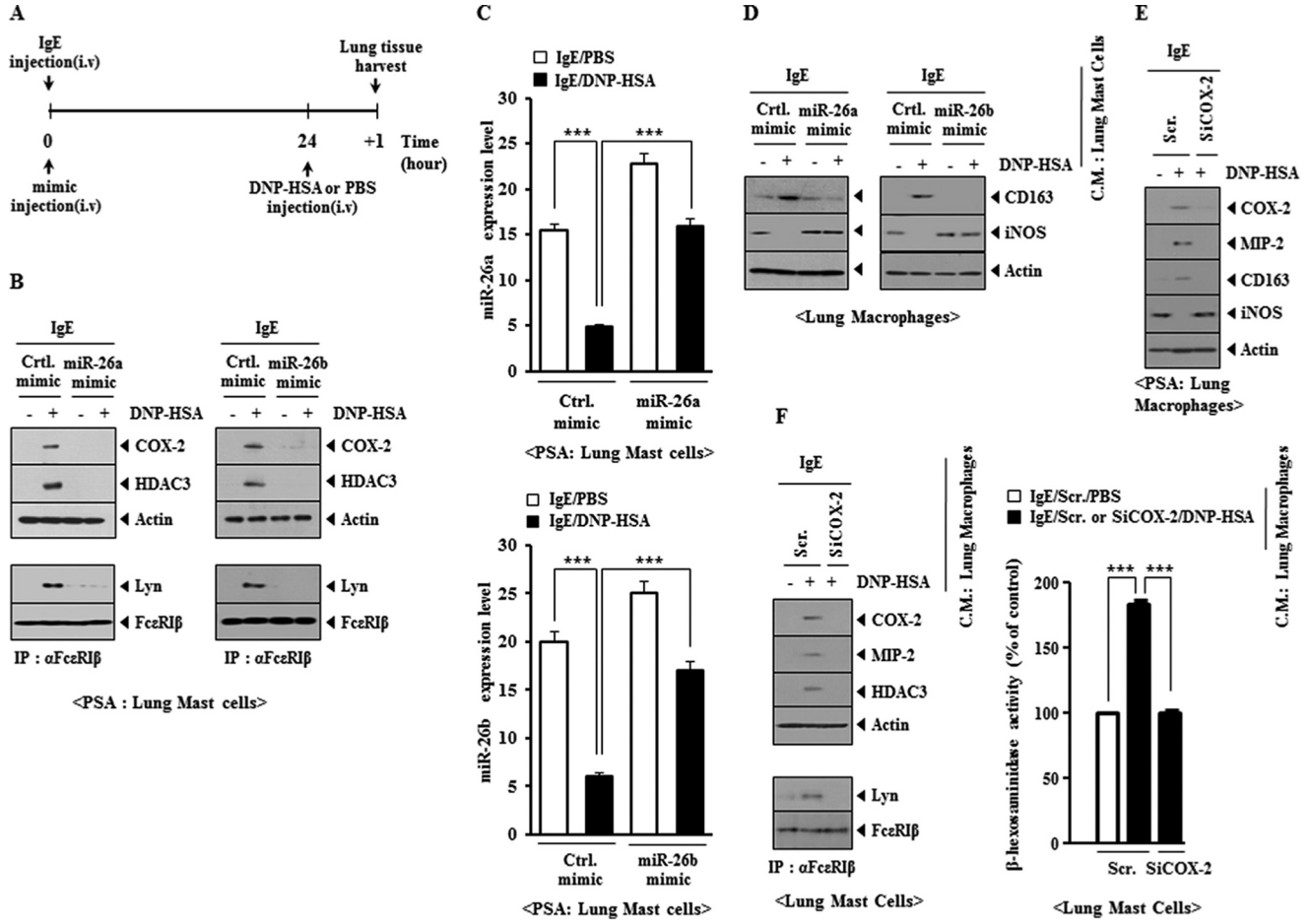

FIGURE 14. **miR-26a mimic and miR-26b mimic prevent an interaction between mast cells and macrophages during allergic inflammation.** *A*, BALB/c mice were given an intravenous (*i.v.*) injection of DNP-specific IgE (0.5 μg/kg) along with miR-26a mimic (100 nM) or miR-26b mimic (100 nM). The next day, BALB/c mice were given an intravenous injection of DNP-HSA (250 μg/kg). One day after the injection of DNP-HSA, lung tissue was harvested. *B*, lung mast cells were isolated from lung tissue, and cell lysates were subjected to Western blot analysis or immunoprecipitated (*IP*) with the indicated antibody, followed by Western blot analysis. *C*, the expression level of miR-26a or miR-26b was also determined by qRT-PCR. ***, $p < 0.0005$. *D*, the conditioned medium of lung mast cells, isolated from each mouse of the experimental group, was added to lung macrophages for 24 h, and Western blot analysis was performed. *E*, BALB/c mice were injected with scrambled (*Scr.*) (100 nM) or COX-2 siRNA (100 nM) via the tail vein. The next day, BALB/c mice were injected with DNP-specific IgE (0.5 μg/kg) via the tail vein. The following day, BALB/c mice were injected intravenously with DNP-HSA (250 μg/kg) or PBS. Two hours after the injection of DNP-HSA, lung macrophage lysates were isolated and subjected to Western blot analysis. *F*, the conditioned medium of lung macrophages after PSA induction was added to lung mast cells for 24 h, followed by Western blot, immunoprecipitation, and β-hexosaminidase activity assays in lung mast cells. ***, $p < 0.0005$. *Error bars*, S.E.

for inflammation-driven angiogenesis and the expression of VEGF-A and VEGFR2 (32). We examined whether PSA-activated mast cells display angiogenic potential. For this, lung mast cells were isolated from lung tissues after PSA in the absence or presence of miR-26a mimic or miR-26b mimic. The conditioned medium was then mixed with Matrigel, and intravital microscopy was performed. Lung mast cells activated by PSA displayed angiogenic potential (Fig. 15*A*). miR-26a mimic and miR-26b mimic exerted negative effects on the angiogenic potential of lung mast cells (Fig. 15*A*). Matrigel plug assays showed that miR-26a mimic and miR-26b mimic negatively regulated the angiogenic potential of lung mast cells (Fig. 15*B*). The addition of conditioned medium of lung mast cells after PSA in the presence of miR-26a mimic or miR-26b mimic mouse lung endothelial cells (*MLECs*) exerted negative effects on the increased expression of HDAC3, COX-2, MIP-2, VEGF-A, and pVEGFR2 in MLECs by PSA (Fig. 15*C*). These results suggest that mast cells, activated by allergic inflammation, promote angiogenesis to drive allergic inflammation-promoted enhanced tumorigenic potential.

COX-2 Is Necessary for the Enhanced Metastatic Potential of Cancer Cells by Allergic Inflammation and for the Interaction between Cancer Cells and Mast Cells—PSA enhanced the metastatic potential of B16F1 melanoma cells in a COX-2-dependent manner (Fig. 16*A*). Western blot analysis of lung tumor tissue showed that PSA increased the expression of HDAC3, COX-2, MIP-2, integrin α_5, and SNAIL in a COX-2-dependent manner (Fig. 16*B*). Immunoprecipitation of lung tumor tissue showed that PSA induced an interaction between $Fc\varepsilon RI_\beta$ and Lyn in a COX-2-dependent manner (Fig. 16*B*). Immunohistochemistry staining of lung tumor tissues showed that PSA induced the expression of COX-2 and MIP-2 in a COX-2-dependent manner (Fig. 16*C*). The increased β-hexosaminidase activity in lung tumor tissue lysates occurred in a COX-2-dependent manner (Fig. 16*D*). These results suggest that the enhanced metastatic potential of cancer cells may result from the interaction between cancer cells and mast cells. We next examined whether cancer cells could activate mast cells. For this, the conditioned medium of B16F10 cells transfected with SiCOX-2 was added to lung mast cells. The down-regulation of

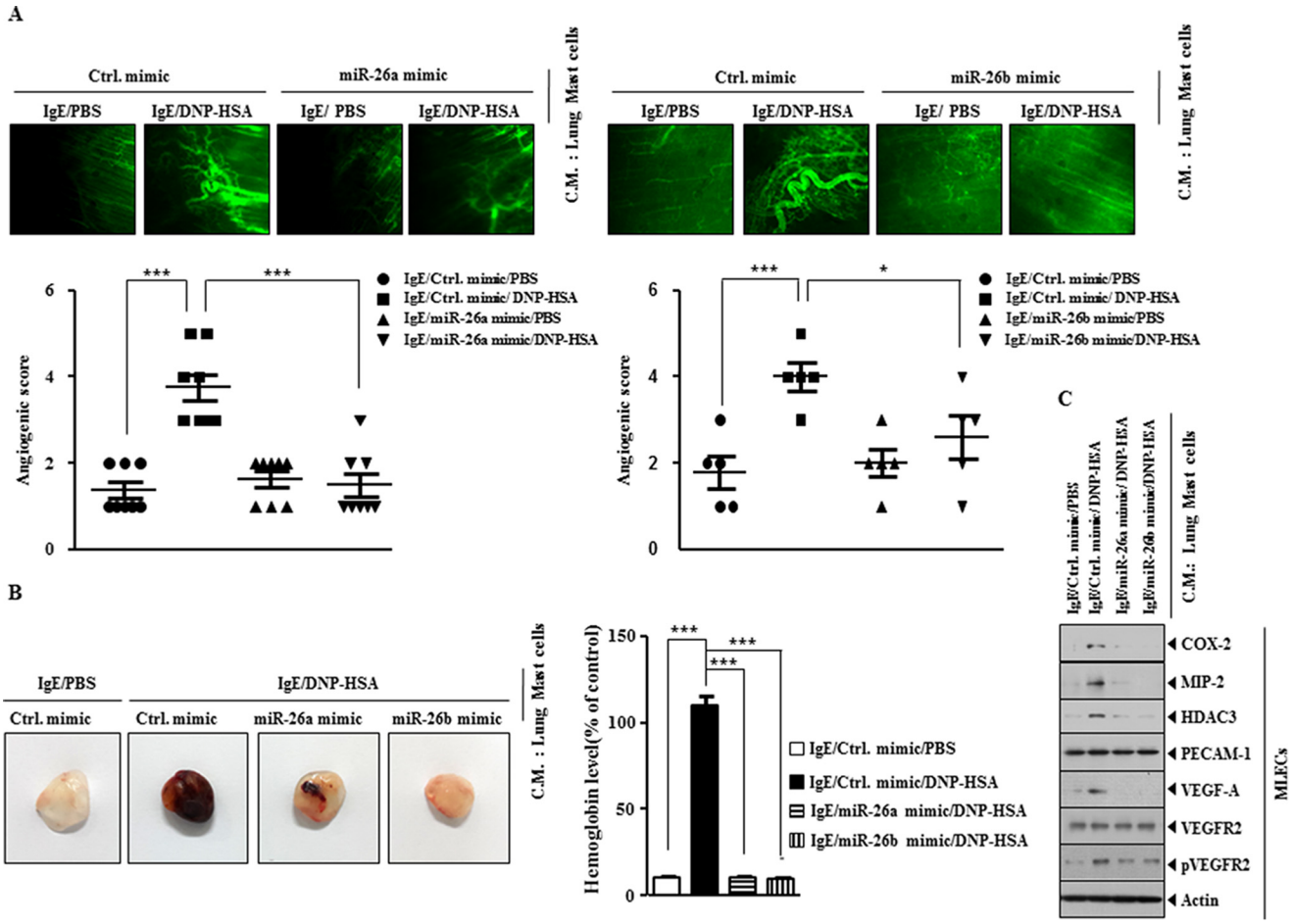

FIGURE 15. **miR-26a mimic and miR-216b mimic negatively regulate PSA-promoted enhanced angiogenic potential of mast cells.** *A*, PSA employing BALB/c mouse was performed in the absence or presence of miR-26a mimic (100 nM) or miR-26 mimic (100 nM). Lung mast cells were isolated from lung tissue. The conditioned medium of lung mast cells was mixed with Matrigel, followed by intravital microscopy performed as described. *, $p < 0.05$; ***, $p < 0.0005$. *B*, same as *A* except that Matrigel plug assays were performed. Hemoglobin content was determined as described. ***, $p < 0.0005$. *C*, the conditioned medium of lung mast cells isolated after PSA in the absence or presence of miR-26a mimic or miR-26 mimic was added to mouse lung endothelial cells (*MLECs*) for 1 h, followed by Western blot analysis. *Error bars*, S.E.

COX-2 decreased the expression of MCP1, HDAC3, TGaseII, integrin α_5, and SNAIL in B16F10 cells (Fig. 16*E*). Lung mast cells showed the increased expression of COX-2 and HDAC3 by the conditioned medium of B16F10 cells (Fig. 16*E*). The addition of conditioned medium of B16F10 cells to lung mast cells increased β-hexosaminidase activity and induced an interaction between FcεRI and Lyn in a COX-2-dependent manner (Fig. 16*F*). These results suggest that COX-2 is necessary for the activation of mast cells by cancer cells in allergic inflammation-promoted enhanced metastatic potential of cancer cells.

Discussion

In this study, we show the role of COX-2 in *in vivo* allergic inflammations, such as PCA, PSA, and TpCR (Fig. 1). The induction of COX-2 in antigen-stimulated RBL2H3 cells occurs at the transcriptional level (Fig. 2*D*). It will be necessary to identify transcriptional factors that regulate the expression of COX-2 during allergic inflammation. EGF induces the expression of COX-2 via SP1 (33). The role of EGFR signaling in allergic inflammation has been reported (34). The inhibition of EGFR signaling may prevent antigen from increasing the expression of COX-2.

TargetScan analysis predicts miR-26a as a negative regulator of IL-6. IgE-mediated activation of mouse bone marrow-derived mast cells enhances calpain activity. Calpain inhibitors block IgE-mediated IL-6 production *in vitro* and reduce late phase allergic response *in vivo* (35). It would be interesting to examine the role of miR-26a and miR-26b on IL-6 expression. TargetScan analysis predicts that miR-26a targets Toll-like receptor 3 (TLR3). TLR3 plays a pivotal role in airway hyperresponsiveness in response to microbial infection in allergic lung inflammation (36). In mice with allergic airway inflammation, dsRNA (a ligand of TLR3) challenge causes a significant exacerbation, increasing lung tissue inflammation score and tissue neutrophilia (37). TLR3 activation induces production of allergen-specific IgE and IgG1 (38). TLR3 null mice shows decreased rhinovirus-induced airway inflammatory and contractile responses (39). Poly(I:C) (TLR3) stimulation increases the secretion of IL-6 and GM-CSF from the nasal mucosa and the epithelial cell lines (40). Based on the above reports, it is probable that *in vivo* allergic inflammation, such as PCA, PSA,

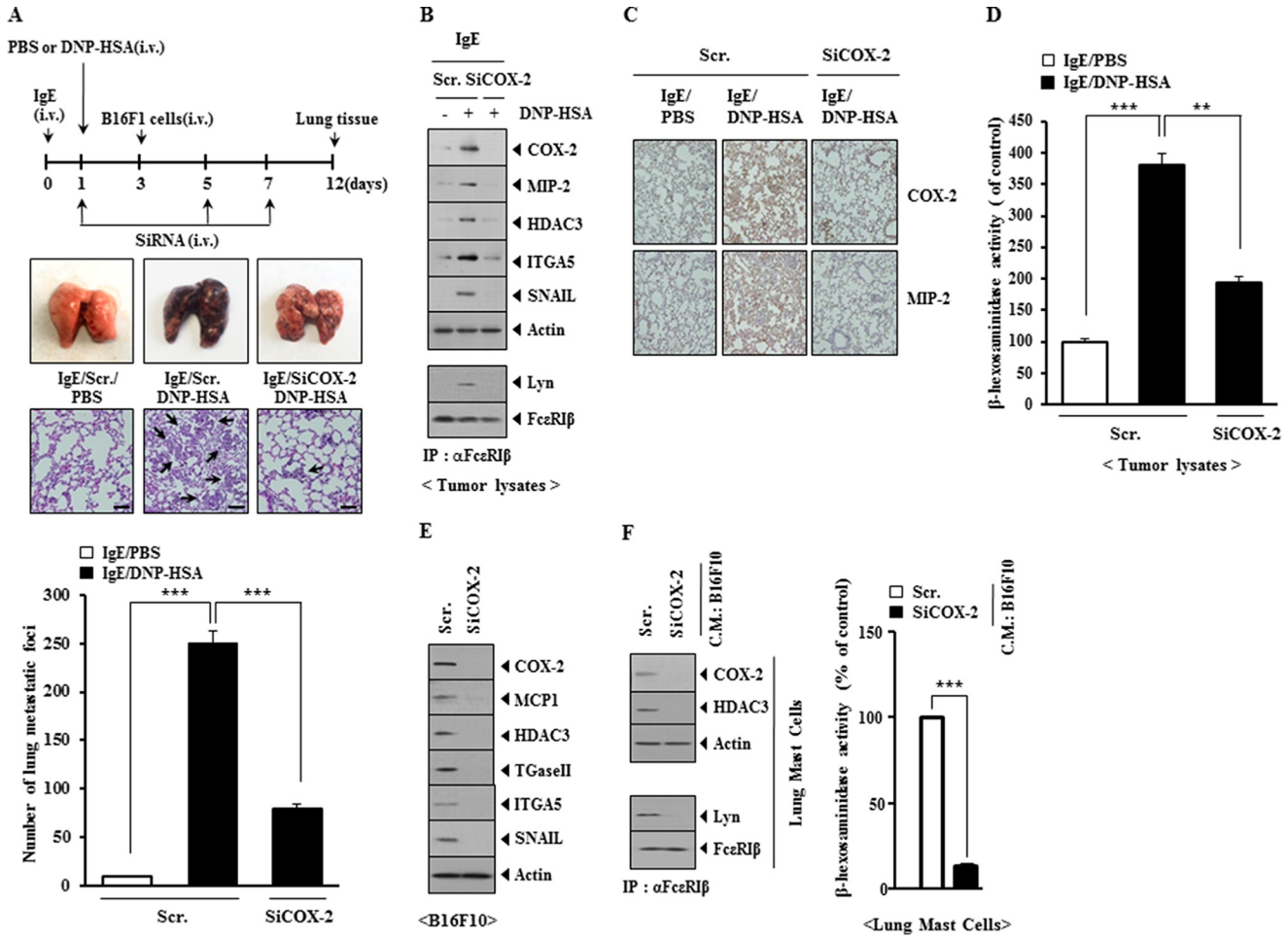

FIGURE 16. **COX-2 is necessary for PSA-promoted enhanced metastatic potential of B16F1 melanoma cells and is necessary for an interaction between cancer cells and mast cells.** *A*, BALB/c mice were sensitized to DNP-specific IgE (0.5 μg/kg) by an intravenous (*i.v.*) injection. The next day, BALB/c mice were given an intravenous injection of DNP-HSA (250 μg/kg). Each mouse received an injection of B16F1 melanoma cells (2×10^5) on day 3 of the time line. BALB/c mice were given an intravenous injection with the indicated siRNA (100 nM) on days 1, 5, and 7 of the time line. On day 12 of the time line, lung tissues were harvested. Formalin-fixed lung sections were stained with H&E. *Black arrows*, lung metastatic foci (*scale bar*, 100 μm). The extent of lung metastasis was determined as described. ***, $p < 0.0005$. *B*, lung tumor tissue lysates were isolated from each mouse of each experimental group of mice and were subjected to Western blot analysis (*top*). Lung tumor lysates isolated from each mouse of each experimental group of mice were immunoprecipitated (*IP*) with the indicated antibody, followed by Western blot analysis (*bottom*). *C*, immunohistochemistry staining employing lung tumor tissues was performed as described. *D*, lung tumor tissue lysates were isolated and subjected to β-hexosaminidase activity assays. **, $p < 0.005$; ***, $p < 0.0005$. *E*, B16F10 cells were transfected with the indicated siRNA (each at 10 nM). At 48 h after transfection, cell lysates were subjected to Western blot analysis. *F*, the conditioned medium of B16F10 cells obtained after transfection with the indicated siRNA was added to lung mast cells. At 24 h after the addition of the conditioned medium, β-hexosaminidase activity assay, Western blot analysis, and immunoprecipitation were performed. ***, $p < 0.0005$. *Error bars*, S.E.

and TpCR, involves the activation of TLR3. It is reasonable that miR-26a negatively regulates TLR3 signaling during allergic inflammations.

TargetScan analysis predicts that miRNAs, such as miR-200a and miR-141, target the expression of MIP-2.[4] miR-200a represses the expression of TGFβ1 and TGFβ2 and regulates TGFβ-dependent epithelial-mesenchymal transition (41). Allergen-induced airway remodeling is mediated by aldose reductase, and its inhibition blocks the progression of remodeling via inhibiting the TGFβ1-induced Smad-independent and PI3K/AKT/GSK3β-dependent pathway (42). The inhibition of aldose reductase prevents ragweed pollen extract-induced increase in COX-2 expression (43). Aldose reductase negatively regulates the expression of miR-200a-3p/141–3p. miR-200a-3p/141-3p, in turn, target Keap1, TGFβ2, and Zeb2 to control renal oxidative stress (44). Because TGFβ signaling is involved in allergic inflammation, it is probable that miR-200a/-141-3p act as a negative regulator of allergic inflammation.

Promoter sequences of miR-26a contain a binding site for transcriptional factors, such as SNAIL, YY1, AP1, Smad, NF-κB, and SP1.[4] The role of SP1 in allergic inflammation has been reported (45). It would be interesting to examine whether SP1 would directly regulate the expression of miR-26a and/or miR-26b in allergic inflammations. Promoter sequences of miR-26b also contain a binding site for SP1 and SNAIL. The role of SNAIL in allergic inflammation has been shown previously (46). We show the binding of SNAIL to the promoter sequences of miR-26a and miR-26b.[4] It would be interesting to examine the potential feedback loop between SP1 and/or SNAIL and miR-26a/-26b.

ChIP assays show the binding of HDAC3 to the promoter sequences of miR-26a and miR-26b.[4] miR-26a and miR-26b

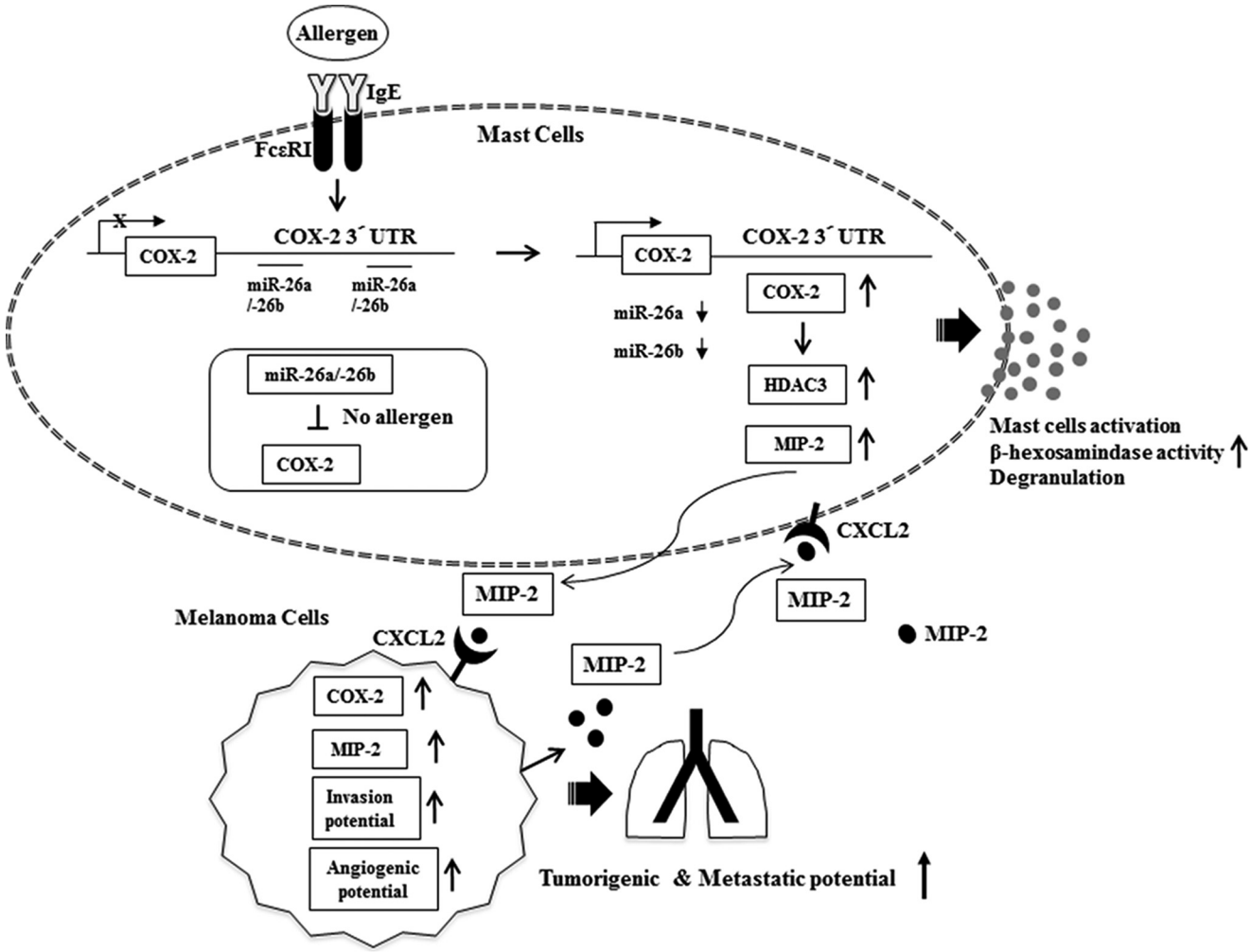

FIGURE 17. **Regulatory role of the miR-26a/-26b-COX-2-MIP-2 loop in allergic inflammation.**

negatively regulate the expression of HDAC3 in allergic inflammation (Fig. 4*B*). This suggests that HDAC3 may form a negative feedback loop with miR-26a/-26b. It is reasonable that HDAC3 may regulate the expression of COX-2.

TGaseII interacts with Rac1 and is responsible for the increased ROS during allergic inflammation (46). Thus, TGaseII may be necessary for the induction of COX-2 by allergic inflammation. miR-26a and miR-26b negatively regulate the expression of TGaseII in antigen-stimulated RBL2H3 cells (Fig. 4*B*). It would be interesting to examine whether miR-26a/-26b form a negative feedback loop with TGaseII.

Low level laser therapy decreases the production of ROS and the expression of MIP-2 in LPS- or H_2O_2-stimulated alveolar macrophages (47). TNF-α mediates cristobalite-induced MCP1 and MIP-2 expression through the generation of ROS in murine alveolar type II cells (48). The above reports are suggestive of a role of miR-26a and miR-26b in the regulation of MIP-2 expression. We show that miR-26a and miR-26b negatively regulate Rac1 activity, ROS production, and the expression of MIP-2 during allergic inflammation (Fig. 4*C*).

Cytokine array analysis shows that the induction of MCP1 and MIP-2 by antigen stimulation occurs in a COX-2-dependent manner (Fig. 7*A*). Mast cells initiate an early phase of neutrophil recruitment by releasing MIP-2 during tissue inflammation (49). MCP1 promotes inflammatory intra-aneurysmal tissue healing in an MIP-2-dependent pathway (50). miR-21 is overexpressed in a mouse model of colitis and is responsible for the increased expression of MIP-2 (51). Because HDAC3 binds to the promoter sequences of MIP-2 (Fig. 9, *B* and *C*), it is reasonable that miR-21 may increase the expression of MIP-2 via HDAC3. Thus, MCP1 increases the expression of HDAC3, which in turn binds to the promoter sequences of MIP-2 to increase the expression of MIP-2.

miR-26b is predicted to target hepatocyte growth factor (HGF). HGF regulates allergic airway inflammation, hyperresponsiveness, and remodeling (52). The HGF-HGRF (HGF receptor) (c-Met) axis regulates the angiogenic potential of human hepatocellular carcinoma (53). In this study, we show that miR-26a and miR-26b regulate the angiogenic potential of the activated mast cells (Fig. 15, *A* and *B*). HGF and miR-26a/-26b probably form a negative feedback loop to regulate allergic inflammation.

Cancer cells are often associated with abundant macrophages that resemble the alternatively activated M2 subset. Tumor-associated macrophages inhibit anti-tumor immune responses and promote metastasis (54). COX-2 inhibition causes loss of the M2 macrophage characteristics of tumor-associated macrophages and prevents breast cancer metastasis

(54). In this study, we show that COX-2 is necessary for allergic inflammation-promoted enhanced metastatic potential of cancer cells (Fig. 16*A*).

In this study, we show that COX-2 regulates allergic inflammation *in vitro* and *in vivo* by forming a negative feedback loop with miR-26a/-26b (Fig. 17). We present evidence that miR-26a and miR-26b regulate the interaction between cancer cells and mast cells and the interaction among stromal cells during allergic inflammation-promoted enhanced tumorigenic and metastatic potential. We show that the induction of MIP-2 occurs in a COX-2-dependent manner during allergic inflammation. Cytokines such as MIP-2 may mediate interactions between cancer cells and stromal cells during allergic inflammation-promoted enhanced tumorigenic potential (Fig. 17). In this study, we show that the miR-26a/-26b-COX-2-MIP-2 loop regulates allergic inflammation and allergic inflammation-promoted enhanced tumorigenic and metastatic potential of cancer cells. The miR-26a/-26b-COX-2-MIP-2 loop may offer a valuable target for the development of anti-allergy and anti-cancer drugs.

References

1. Jeon, C. M., Shin, I. S., Shin, N. R., Hong, J. M., Kwon, O. K., Kim, H. S., Oh, S. R., Myung, P. K., and Ahn, K. S. (2014) *Siegesbeckia glabrescens* attenuates allergic airway inflammation in LPS-stimulated RAW 264.7 cells and OVA induced asthma murine model. *Int. Immunopharmacol.* **22,** 414–419
2. Huang, W. C., Chai, C. Y., Chen, W. C., Hou, M. F., Wang, Y. S., Chiu, Y. C., Lu, S. R., Chang, W. C., Juo, S. H., Wang, J. Y., and Chang, W. C. (2011) Histamine regulates cyclooxygenase 2 gene activation through Orai1-mediated NFκB activation in lung cancer cells. *Cell Calcium* **50,** 27–35
3. Shiraishi, Y., Asano, K., Niimi, K., Fukunaga, K., Wakaki, M., Kagyo, J., Takihara, T., Ueda, S., Nakajima, T., Oguma, T., Suzuki, Y., Shiomi, T., Sayama, K., Kagawa, S., Ikeda, E., Hirai, H., Nagata, K., Nakamura, M., Miyasho, T., and Ishizaka, A. (2008) Cyclooxygenase-2/prostaglandin D2/CRTH2 pathway mediates double-stranded RNA-induced enhancement of allergic airway inflammation. *J. Immunol.* **180,** 541–549
4. Passos, G. F., Medeiros, R., Marcon, R., Nascimento, A. F., Calixto, J. B., and Pianowski, L. F. (2013) The role of PKC/ERK1/2 signaling in the anti-inflammatory effect of tetracyclic triterpene euphol on TPA-induced skin inflammation in mice. *Eur. J. Pharmacol.* **698,** 413–420
5. Morin, C., Fortin, S., Cantin, A. M., and Rousseau, É. (2013) MAG-EPA resolves lung inflammation in an allergic model of asthma. *Clin. Exp. Allergy* **43,** 1071–1082
6. Li, H., Edin, M. L., Bradbury, J. A., Graves, J. P., DeGraff, L. M., Gruzdev, A., Cheng, J., Dackor, R. T., Wang, P. M., Bortner, C. D., Garantziotis, S., Jetten, A. M., and Zeldin, D. C. (2013) Cyclooxygenase-2 inhibits T helper cell type 9 differentiation during allergic lung inflammation via down-regulation of IL-17RB. *Am. J. Respir. Crit. Care Med.* **187,** 812–822
7. Church, R. J., Jania, L. A., and Koller, B. H. (2012) Prostaglandin E(2) produced by the lung augments the effector phase of allergic inflammation. *J. Immunol.* **188,** 4093–4102
8. Dohadwala, M., Yang, S. C., Luo, J., Sharma, S., Batra, R. K., Huang, M., Lin, Y., Goodglick, L., Krysan, K., Fishbein, M. C., Hong, L., Lai, C., Cameron, R. B., Gemmill, R. M., Drabkin, H. A., and Dubinett, S. M. (2006) Cyclooxygenase-2-dependent regulation of E-cadherin: prostaglandin E(2) induces transcriptional repressors ZEB1 and snail in non-small cell lung cancer. *Cancer Res.* **66,** 5338–5345
9. Eom, S., Kim, Y., Kim, M., Park, D., Lee, H., Lee, Y. S., Choe, J., Kim, Y. M., and Jeoung, D. (2014) Transglutaminase II/miR-218/-181a loop regulates positive feedback relationship between allergic inflammation and tumor metastasis. *J. Biol. Chem.* **289,** 29483–29505
10. Eom, S., Kim, Y., Park, D., Lee, H., Lee, Y. S., Choe, J., Kim, Y. M., and Jeoung, D. (2014) Histone deacetylase-3 mediates positive feedback relationship between anaphylaxis and tumor metastasis. *J. Biol. Chem.* **289,** 12126–12144
11. Olivera, A., Dillahunt, S. E., and Rivera, J. (2013) Interrogation of sphingosine-1-phosphate receptor 2 function *in vivo* reveals a prominent role in the recovery from IgE- and IgG-mediated anaphylaxis with minimal effect on its onset. *Immunol. Lett.* **150,** 89–96
12. Cao, D., Bromberg, P. A., and Samet, J. M. (2007) COX-2 expression induced by diesel particles involves chromatin modification and degradation of HDAC1. *Am. J. Respir. Cell Mol. Biol.* **37,** 232–239
13. McKinley, L., Kim, J., Bolgos, G. L., Siddiqui, J., and Remick, D. G. (2005) CXC chemokines modulate IgE secretion and pulmonary inflammation in a model of allergic asthma. *Cytokine* **32,** 178–185
14. Fogli, L. K., Sundrud, M. S., Goel, S., Bajwa, S., Jensen, K., Derudder, E., Sun, A., Coffre, M., Uyttenhove, C., Van Snick, J., Schmidt-Supprian, M., Rao, A., Grunig, G., Durbin, J., Casola, S. S., Rajewsky, K., and Koralov, S. B. (2013) T cell-derived IL-17 mediates epithelial changes in the airway and drives pulmonary neutrophilia. *J. Immunol.* **191,** 3100–3111
15. Nagarkar, D. R., Wang, Q., Shim, J., Zhao, Y., Tsai, W. C., Lukacs, N. W., Sajjan, U., and Hershenson, M. B. (2009) CXCR2 is required for neutrophilic airway inflammation and hyperresponsiveness in a mouse model of human rhinovirus infection. *J. Immunol.* **183,** 6698–6707
16. Lappalainen, U., Whitsett, J. A., Wert, S. E., Tichelaar, J. W., and Bry, K. (2005) Interleukin-1β causes pulmonary inflammation, emphysema, and airway remodeling in the adult murine lung. *Am. J. Respir. Cell Mol. Biol.* **32,** 311–318
17. Bartel, D. P. (2009) MicroRNAs: target recognition and regulatory functions. *Cell* **136,** 215–233
18. Fabian, M. R., Sonenberg, N., and Filipowicz, W. (2010) Regulation of mRNA translation and stability by microRNAs. *Ann. Rev. Biochem.* **79,** 351–379
19. Rebane, A., Runnel, T., Aab, A., Maslovskaja, J., Rückert, B., Zimmermann, M., Plaas, M., Kärner, J., Treis, A., Pihlap, M., Haljasorg, U., Hermann, H., Nagy, N., Kemeny, L., Erm, T., Kingo, K., Li, M., Boldin, M. P., and Akdis, C. A. (2014) MicroRNA-146a alleviates chronic skin inflammation in atopic dermatitis through suppression of innate immune responses in keratinocytes. *J. Allergy Clin. Immunol.* **134,** 836–847.e11
20. Xiang, Y., Eyers, F., Young, I. G., Rosenberg, H. F., Foster, P. S., and Yang, M. (2014) Identification of microRNAs regulating the developmental pathways of bone marrow derived mast cells. *PLoS One* **9,** e98139
21. Yang, M., Eyers, F., Xiang, Y., Guo, M., Young, I. G., Rosenberg, H. F., and Foster, P. S. (2014) Expression profiling of differentiating eosinophils in bone marrow cultures predicts functional links between microRNAs and their target mRNAs. *PLoS One* **9,** e97537
22. Yamada, Y., Kosaka, K., Miyazawa, T., Kurata-Miura, K., and Yoshida, T. (2014) miR-142–3p enhances FcεRI-mediated degranulation in mast cells. *Biochem. Biophys. Res. Commun.* **443,** 980–986
23. Collison, A., Mattes, J., Plank, M., and Foster, P. S. (2011) Inhibition of house dust mite-induced allergic airways disease by antagonism of microRNA-145 is comparable to glucocorticoid treatment. *J. Allergy Clin. Immunol.* **128,** 160–167.e4
24. Polikepahad, S., Knight, J. M., Naghavi, A. O., Oplt, T., Creighton, C. J., Shaw, C., Benham, A. L., Kim, J., Soibam, B., Harris, R. A., Coarfa, C., Zariff, A., Milosavljevic, A., Batts, L. M., Kheradmand, F., Gunaratne, P. H., and Corry, D. B. (2010) Proinflammatory role for let-7 microRNAS in experimental asthma. *J. Biol. Chem.* **285,** 30139–30149
25. Mattes, J., Collison, A., Plank, M., Phipps, S., and Foster, P. S. (2009) Antagonism of microRNA-126 suppresses the effector function of TH2 cells and the development of allergic airways disease. *Proc. Natl. Acad. Sci. U.S.A.* **106,** 18704–18709
26. Wu, F., Zikusoka, M., Trindade, A., Dassopoulos, T., Harris, M. L., Bayless, T. M., Brant, S. R., Chakravarti, S., and Kwon, J. H. (2008) MicroRNAs are differentially expressed in ulcerative colitis and alter expression of macrophage inflammatory peptide-2α. *Gastroenterology* **135,** 1624–1635.e24
27. Kim, Y., Lee, Y. S., Hahn, J. H., Choe, J., Kwon, H. J., Ro, J. Y., and Jeoung, D. (2008) Hyaluronic acid targets CD44 and inhibits FcepsilonRI signaling involving PKCδ, Rac1, ROS, and MAPK to exert anti-allergic effect. *Mol. Immunol.* **45,** 2537–2547

28. Kim, Y., Kim, K., Park, D., Lee, E., Lee, H., Lee, Y. S., Choe, J., and Jeoung, D. (2012) Histone deacetylase 3 mediates allergic skin inflammation by regulating expression of MCP1 protein. *J. Biol. Chem.* **287,** 25844–25859
29. Aung, H. T., Schroder, K., Himes, S. R., Brion, K., van Zuylen, W., Trieu, A., Suzuki, H., Hayashizaki, Y., Hume, D. A., Sweet, M. J., and Ravasi, T. (2006) LPS regulates proinflammatory gene expression in macrophages by altering histone deacetylase expression. *FASEB J.* **20,** 1315–1327
30. Ano, S., Morishima, Y., Ishii, Y., Yoh, K., Yageta, Y., Ohtsuka, S., Matsuyama, M., Kawaguchi, M., Takahashi, S., and Hizawa, N. (2013) Transcription factors GATA-3 and RORγt are important for determining the phenotype of allergic airway inflammation in a murine model of asthma. *J. Immunol.* **190,** 1056–1065
31. Rose, C. E. Jr., Lannigan, J. A., Kim, P., Lee, J. J., Fu, S. M., and Sung, S. S. (2010) Murine lung eosinophil activation and chemokine production in allergic airway inflammation. *Cell. Mol. Immunol.* **7,** 361–374
32. Davaatseren, M., Hwang, J. T., Park, J. H., Kim, M. S., Wang, S., and Sung, M. J. (2014) Allyl isothiocyanate ameliorates angiogenesis and inflammation in dextran sulfate sodium-induced acute colitis. *PLoS One* **9,** e102975
33. Xu, K., and Shu, H. K. (2013) Transcription factor interactions mediate EGF-dependent COX-2 expression. *Mol. Cancer Res.* **11,** 875–886
34. Kim, Y., Kim, K., Park, D., Eom, S., Park, H., Lee, H., Lee, Y. S., Choe, J., Hahn, J. H., Kim, Y. M., Ro, J. Y., and Jeoung, D. (2011) Integrin α(5) interacts with EGFR, is necessary for FcεRI signaling and is necessary for allergic inflammation in relation with angiogenesis. *Mol. Immunol.* **48,** 1035–1045
35. Wu, Z., Chen, X., Liu, F., Chen, W., Wu, P., Wieschhaus, A. J., Chishti, A. H., Roche, P. A., Chen, W. M., and Lin, T. J. (2014) Calpain-1 contributes to IgE-mediated mast cell activation. *J. Immunol.* **192,** 5130–5139
36. Starkhammar, M., Larsson, O., Kumlien Georén, S., Leino, M., Dahlén, S. E., Adner, M., and Cardell, L. O. (2014) Toll-like receptor ligands LPS and poly(I:C) exacerbate airway hyperresponsiveness in a model of airway allergy in mice, independently of inflammation. *PLoS One* **9,** e104114
37. Mahmutovic-Persson, I., Akbarshahi, H., Bartlett, N. W., Glanville, N., Johnston, S. L., Brandelius, A., and Uller, L. (2014) Inhaled dsRNA and rhinovirus evoke neutrophilic exacerbation and lung expression of thymic stromal lymphopoietin in allergic mice with established experimental asthma. *Allergy* **69,** 348–358
38. Reuter, S., Dehzad, N., Martin, H., Böhm, L., Becker, M., Buhl, R., Stassen, M., and Taube, C. (2012) TLR3 but not TLR7/8 ligand induces allergic sensitization to inhaled allergen. *J. Immunol.* **188,** 5123–5131
39. Wang, Q., Miller, D. J., Bowman, E. R., Nagarkar, D. R., Schneider, D., Zhao, Y., Linn, M. J., Goldsmith, A. M., Bentley, J. K., Sajjan, U. S., and Hershenson, M. B. (2011) MDA5 and TLR3 initiate pro-inflammatory signaling pathways leading to rhinovirus-induced airways inflammation and hyperresponsiveness. *PLoS Pathog.* **7,** e1002070
40. Tengroth, L., Millrud, C. R., Kvarnhammar, A. M., Kumlien Georén, S., Latif, L., Cardell, L. O. (2014) Functional effects of Toll-like receptor (TLR)3, 7, 9, RIG-I and MDA-5 stimulation in nasal epithelial cells. *PLoS One* **9,** e98239
41. Wang, B., Koh, P., Winbanks, C., Coughlan, M. T., McClelland, A., Watson, A., Jandeleit-Dahm, K., Burns, W. C., Thomas, M. C., Cooper, M. E., and Kantharidis, P. (2011) miR-200a prevents renal fibrogenesis through repression of TGF-β2 expression. *Diabetes* **60,** 280–287
42. Yadav, U. C., Naura, A. S., Aguilera-Aguirre, L., Boldogh, I., Boulares, H. A., Calhoun, W. J., Ramana, K. V., and Srivastava, S. K. (2013) Aldose reductase inhibition prevents allergic airway remodeling through PI3K/AKT/GSK3β pathway in mice. *PLoS One* **8,** e57442
43. Yadav, U. C., Ramana, K. V., Aguilera-Aguirre, L., Boldogh, I., Boulares, H. A., and Srivastava, S. K. (2009) Inhibition of aldose reductase prevents experimental allergic airway inflammation in mice. *PLoS One* **4,** e6535
44. Wei, J., Zhang, Y., Luo, Y., Wang, Z., Bi, S., Song, D., Dai, Y., Wang, T., Qiu, L., Wen, L., Yuan, L., and Yang, J. Y. (2014) Aldose reductase regulates miR-200a-3p/141–3p to coordinate Keap1-Nrf2, Tgfβ1/2, and Zeb1/2 signaling in renal mesangial cells and the renal cortex of diabetic mice. *Free Radic. Biol. Med.* **67,** 91–102
45. Maeda, K., Nishiyama, C., Ogawa, H., and Okumura, K. (2010) GATA2 and Sp1 positively regulate the c-kit promoter in mast cells. *J. Immunol.* **185,** 4252–4260
46. Kim, Y., Eom, S., Kim, K., Lee, Y. S., Choe, J., Hahn, J. H., Lee, H., Kim, Y. M., Ha, K. S., Ro, J. Y., and Jeoung, D. (2010) Transglutaminase II interacts with rac1, regulates production of reactive oxygen species, expression of snail, secretion of Th2 cytokines and mediates *in vitro* and *in vivo* allergic inflammation. *Mol. Immunol.* **47,** 1010–1022
47. de Lima, F. M., Villaverde, A. B., Albertini, R., de Oliveira, A. P., Faria Neto, H. C., and Aimbire, F. (2010) Low-level laser therapy associated to *N*-acetylcysteine lowers macrophage inflammatory protein-2 (MIP-2) mRNA expression and generation of intracellular reactive oxygen species in alveolar macrophages. *Photomed. Laser Surg.* **28,** 763–771
48. Barrett, E. G., Johnston, C., Oberdörster, G., and Finkelstein, J. N. (1999) Silica-induced chemokine expression in alveolar type II cells is mediated by TNF-α-induced oxidant stress. *Am. J. Physiol.* **276,** 979–988
49. De Filippo, K., Dudeck, A., Hasenberg, M., Nye, E., van Rooijen, N., Hartmann, K., Gunzer, M., Roers, A., and Hogg, N. (2013) Mast cell and macrophage chemokines CXCL1/CXCL2 control the early stage of neutrophil recruitment during tissue inflammation. *Blood* **121,** 4930–4937
50. Hoh, B. L., Hosaka, K., Downes, D. P., Nowicki, K. W., Fernandez, C. E., Batich, C. D., and Scott, E. W. (2011) Monocyte chemotactic protein-1 promotes inflammatory vascular repair of murine carotid aneurysms via a macrophage inflammatory protein-1α and macrophage inflammatory protein-2-dependent pathway. *Circulation* **124,** 2243–2252
51. Shi, C., Liang, Y., Yang, J., Xia, Y., Chen, H., Han, H., Yang, Y., Wu, W., Gao, R., and Qin, H. (2013) MicroRNA-21 knockout improve the survival rate in DSS induced fatal colitis through protecting against inflammation and tissue injury. *PLoS One* **8,** e66814
52. Ito, W., Kanehiro, A., Matsumoto, K., Hirano, A., Ono, K., Maruyama, H., Kataoka, M., Nakamura, T., Gelfand, E. W., and Tanimoto, M. (2005) Hepatocyte growth factor attenuates airway hyperresponsiveness, inflammation, and remodeling. *Am. J. Respir. Cell Mol. Biol.* **32,** 268–280
53. Yang, X., Zhang, X. F., Lu, X., Jia, H. L., Liang, L., Dong, Q. Z., Ye, Q. H., and Qin, L. X. (2014) MicroRNA-26a suppresses angiogenesis in human hepatocellular carcinoma by targeting hepatocyte growth factor-cMet pathway. *Hepatology* **59,** 1874–1885
54. Na, Y. R., Yoon, Y. N., Son, D. I., and Seok, S. H. (2013) Cyclooxygenase-2 inhibition blocks M2 macrophage differentiation and suppresses metastasis in murine breast cancer model. *PLoS One* **8,** e63451